The Mesozoic tectono-magmatic evolution at the Paleo-Pacific subduction zone in West Borneo

Juliane Hennig*, H. Tim Breitfeld, Robert Hall and A. M. Surya Nugraha

SE Asia Research Group, Department of Earth Sciences, Royal Holloway University of London, Egham, TW20 0EX, UK

** Corresponding author (e-mail: juliane.hennig@rhul.ac.uk)*

Abstract

Metamorphic and magmatic rocks are present in the northwestern part of the Schwaner Mountains of West Kalimantan. This area was previously assigned to SW Borneo (SWB) and interpreted as an Australian-origin block. Predominantly Cretaceous U-Pb zircon ages (c. 80-130 Ma) have been obtained from metapelites and I-type granitoids in the North Schwaner Zone of the SWB but a Triassic metatonalite discovered in West Kalimantan near Pontianak is inconsistent with a SWB origin. The distribution and significance of Triassic rocks was not known so the few exposures in the Pontianak area were sampled and geochemical analyses and zircon U-Pb ages were obtained from two meta-igneous rocks and three granitoids and diorites. Triassic and Jurassic magmatic and metamorphic zircons obtained from the meta-igneous rocks are interpreted to have formed at the Mesozoic Paleo-Pacific margin where there was subduction beneath the Indochina–East Malaya block. Geochemically similar rocks of Triassic age exposed in the Embuoi Complex to the north and the Jagoi Granodiorite in West Sarawak are suggested to have formed part of the southeastern margin of Triassic Sundaland. One granitoid (118.6 ± 1.1 Ma) has an S-type character and contains inherited Carboniferous, Triassic and Jurassic zircons which indicate that it intruded Sundaland basement. Two I-type granitoids and diorites yielded latest Early and Late Cretaceous weighted mean ages of 101.5 ± 0.6 and 81.1 ± 1.1 Ma. All three magmatic rocks are in close proximity to the meta-igneous rocks and are interpreted to record Cretaceous magmatism at the Paleo-Pacific subduction margin. Cretaceous zircons of metamorphic origin indicate recrystallisation at c. 90 Ma possibly related to the collision of the Argo block with

Sundaland. Subduction ceased at that time, followed by post-collisional magmatism in the Pueh (77.2 ± 0.8 Ma) and Gading Intrusions (79.7 ± 1.0 Ma) of West Sarawak.

Keywords: SE Asia; West Borneo; SW Borneo block; U-Pb zircon geochronology; Paleo-Pacific subduction

1. Introduction

The island of Borneo is divided into Indonesian Kalimantan which includes the western, southern, central and eastern region, the Malaysian states of Sarawak and Sabah that cover most of the northwest and northern areas, and the independent nation of Brunei (Fig. 1a).

The Schwaner Mountains form a 1 to 2 km high mountain range in the southwestern part of Borneo (Fig. 1a, b). Only limited dating has been carried out on the (meta-) igneous rocks in that region and most of the reported ages are based on the K-Ar method which yielded ages ranging from 65 to 130 Ma (Haile et al., 1977; Bladon et al., 1989; Amiruddin & Trail, 1993; De Keyser & Rustandi, 1993; Pieters & Sanyoto, 1993). Widespread metamorphic rocks in the northern zone were assigned to the Pinoh Metamorphics (Fig. 2) which for many years were assumed to be Paleozoic (van Bemmelen, 1949; Haile, 1974; Tate, 1991) to Triassic (Pieters & Sanyoto, 1993), and interpreted to represent old continental basement (van Bemmelen, 1949; Haile, 1974; Metcalfe, 1988). However, U-Pb zircon dating of metapelites from the Pinoh Metamorphic Group revealed Early Cretaceous volcanogenic protoliths (c. 130 Ma) which were subsequently metamorphosed due to the emplacement of the Schwaner intrusions in the Cretaceous between c. 80 and 120 Ma (Davies, 2013; Davies et al., 2014).

More recently, one metatonalite sampled by Setiawan et al. (2013) from southeast of Pontianak has been dated as Triassic (233 ± 3 Ma) by U-Pb zircon LA-ICP-MS (Fig. 2). This age is similar to K-Ar ages reported by Williams et al. (1988) from rocks of the Embuoi Complex in NW Kalimantan (c. 201 to 263 Ma) and zircon U-Pb ages obtained from the Jagoi Granodiorite (c. 208 Ma) in West Sarawak (Breitfeld et al., 2017) in the basement of the Kuching Zone (Haile, 1974) (Fig. 1a, b).

The Triassic magmatism has been related to subduction beneath the eastern Sundaland margin in the Triassic (Breitfeld et al., 2017). The boundary of the Triassic rocks with Cretaceous rocks to the east in the Schwaner Mountains can therefore define the southernmost extent of Triassic Sundaland and the western boundary of the SW Borneo block. Mesozoic magmatic episodes identified in this study are used to further reconstruct the tectonic evolution at the southern Paleo-Pacific subduction margin in West Borneo.

2. Geological background

2.1 Mesozoic in West Borneo

2.1.1 Triassic magmatism

The Embuoi Complex is exposed between the western part of West Sarawak and the Schwaner Mountains (Fig. 1b). It is composed of igneous rocks which are partly foliated and dated as Triassic (c. 201 - 263 Ma) by the K-Ar method (Williams et al., 1988; Supriatna et al., 1993), and interpreted to record pre-Triassic or Triassic magmatism and subsequent deformation.

Similar metamorphic rocks with K-Ar ages of c. 207 - 235 Ma (Bladon et al., 1989) are exposed further east in the Busang Complex (Fig. 1b). However, they are potentially allochthonous fragments in a melange (Tate, 1991; Pieters et al., 1993) which forms inliers in the Cretaceous Selangkai Formation (Heryanto & Jones, 1996).

A Triassic age for the Jagoi Granodiorite in West Sarawak has been confirmed by recent U-Pb zircon dating which yielded an age of 208.3 ± 0.9 Ma, and therefore the western part of the Kuching Zone, including NW Kalimantan and the western part of West Sarawak (Fig. 1b) has been assigned to Triassic Sundaland (Breitfeld et al., 2017). To the northeast and east of the Jagoi Granodiorite, Breitfeld et al. (2017) reported similar Late Triassic white mica Ar-Ar ages (c. 217 and 220 Ma) from schists south of Kuching which are interpreted as metamorphic ages associated with Triassic magmatism.

The Triassic (meta-) igneous rocks are attributed to westward subduction of the Paleo-Pacific plate beneath the eastern Sundaland margin (Breitfeld et al., 2017). Other remnants of this magmatism are the Triassic Serian Volcanic Formation (Pimm, 1965; Wilford & Kho, 1965; JICA, 1985; Bladon et al., 1989; Breitfeld et al., 2017) and the volcaniclastic sediments of the Sadong and Kuching Formations (Wilford & Kho, 1965; Kon`no, 1972; Breitfeld et al., 2017) (Fig. 1b). They form a Triassic basement in Sundaland which is in places overlain by the Jurassic Bau Limestone Formation (Wolfenden, 1965; Bayliss, 1966; Yanagida & Lau, 1978; Beauvais & Fontaine, 1990; Ting, 1992), as well as the Jurassic to Cretaceous Pedawan Formation (Wilford & Kho, 1965; Muller, 1968; Nuraiteng & Kushairi, 1987; Morley, 1998; Basir & Uyop, 1999) (Fig. 1b).

In West Kalimantan igneous rocks of the Embuoi Complex and volcanic rocks of the Jambu Volcanics may represent the Triassic equivalents of the Serian Volcanics (Tate, 1991; Supriatna et al., 1993), and are overlain by limestones and calcareous shales of the upper Middle Jurassic Brandung Formation (Schairer & Zeiss, 1992) (Fig. 1b) which resemble the Bau Limestone Formation in West Sarawak. This suggests that Triassic basement overlain by Jurassic sediments can be traced from West Sarawak to West Kalimantan. The Triassic metatonalite of Setiawan et al. (2013) with a zircon U-Pb weighted mean age of 233 ± 3 Ma indicates a Sundaland affiliation for the northwestern part of the Schwaner Mountains east of Pontianak. However, the boundary between the Triassic basement of Sundaland and the Cretaceous SW Borneo block has not been identified.

2.1.2 Jurassic magmatism

Few magmatic rocks of Jurassic age have been reported from the Schwaner Mountains (Davies, 2013; Davies et al., 2014). One alkaline within-plate granite from the western Schwaner Mountains in the South Schwaner Zone (SSZ) yielded a zircon U-Pb age of 186.7 ± 2.3 Ma (Davies et al., 2014) (Fig. 2). This is similar to a c. 153 Ma K-Ar age from a granite reported by Haile et al. (1977), and a c. 152 Ma age from a zircon core obtained from another SSZ granite of the Ketapang area (Fig. 1a) (van Hattum et al., 2013). There was rifting during the Late Triassic to Late Jurassic at the NW margin of Australia (e.g. Longley et al., 2002) and the Jurassic magmatism of within-plate character was interpreted by Davies

125 (2013) to be related to extension during separation of the SW Borneo block from the
126 Australian margin of Gondwana.
127
128 ***2.1.3 Cretaceous magmatism***
129 Magmatism in the Cretaceous formed the North Schwaner Zone (NSZ) in SW Borneo.
130 Granitoids were assigned mainly to the Sepauk Tonalite and subordinate Laur Granite (Fig.
131 2) on the geological map of Pieters & Sanyoto (1993). They were dated as Cretaceous (c. 75
132 to 130 Ma) by K-Ar analysis (Haile et al., 1977; Bladon et al., 1989; Pieters & Sanyoto, 1993).
133 The wide range of ages was broadly confirmed by zircon U-Pb dating of granitoids from the
134 NSZ which yielded ages between c. 80 Ma and 120 Ma (Davies et al., 2014).
135
136 The Pinoh Metamorphic Group (Fig. 2) in the NSZ was previously assumed to represent
137 basement rocks of Paleozoic (van Bemmelen, 1949; Haile, 1974; Tate, 1991) to Triassic age
138 (Pieters & Sanyoto, 1993). However, all metamorphic rocks dated from the Pinoh
139 Metamorphic Group contain zircons with Early Cretaceous U-Pb ages of ~130 Ma,
140 interpreted to represent volcanogenic protoliths which were subsequently metamorphosed
141 due to the emplacement of the Schwaner intrusions in the Cretaceous between c. 80 Ma
142 and 120 Ma (Davies, 2013; Davies et al., 2014).
143
144 The Sukadana Granite (Fig. 2) is exposed mainly in the South Schwaner Zone (SSZ) (Pieters &
145 Sanyoto, 1993) and yielded Late Cretaceous mineral and whole rock K-Ar ages ranging from
146 c. 65 to 103 Ma, including the youngest ages reported at c. 65 to 74 Ma which were
147 obtained from dykes (De Keyser & Rustandi, 1993). The rocks were interpreted to have been
148 emplaced after subduction had ceased (Amiruddin & Trail, 1993), although they include
149 rocks with ages ranging from 86 to 103 Ma (De Keyser & Rustandi, 1993) very similar to the
150 youngest phase of subduction-related magmatism identified by Davies et al. (2014) in the
151 NSZ. Van Hattum et al. (2013) reported monzogranites with weighted mean ages of 81.7 ±
152 1.0 Ma and 84.7 ± 1.3 Ma from the Sukadana Granite in the Ketapang area. One granite
153 from the SSZ interpreted as post-collisional based on an alkaline character and within-plate
154 signature (Davies et al., 2014) gave a Late Cretaceous weighted mean age of 72.1 ± 0.6 Ma
155 (Fig. 2) from zircon U-Pb dating.

Kirk (1968) reported Upper Cretaceous intrusions from Gunung Gading, Gunung Pueh, Tanjong Datu and Tinteng Bedil in West Sarawak (Fig. 1b). The Gading, Tanjong Datu and Tinteng Bedil Intrusions yielded biotite K-Ar ages ranging from 76 ± 4 Ma to 79 ± 5 Ma (Kirk, 1968). A similar age was inferred for the nearby Pueh Intrusion based on lithological and geochemical similarities (Kirk, 1968). Williams et al. (1988) reported K-Ar ages between c. 75 and 81 Ma from biotite and hornblende in granitoids from the Kuching Zone and interpreted them as post-collisional. The similarities of Upper Cretaceous granitoids in West Sarawak and West Kalimantan suggest a similar tectonic history for these two regions during the Late Cretaceous.

2.2 Tectonic evolution of western Borneo

The origin of west Borneo is still poorly known. Some authors have proposed a Cathaysian affinity for SW Borneo (e.g. Ben-Avraham & Uyeda, 1973). Cathaysian terranes started to rift from the Gondwana supercontinent in the Devonian which opened the Paleo-Tethys. They were accreted to Eurasia in the Carboniferous (Metcalfe, 2009, 2011). During the Permian West Burma, West Sumatra, South China and Indochina-East Malaya formed Cathaysia which was situated in warm equatorial water and climatic conditions, resulting in changing ecosystems and the formation of a distinctive Cathaysian flora and fauna (Metcalfe, 2009, 2011).

Permian and Triassic Cathaysian faunas were identified in the Sadong Formation in West Sarawak (Kon`no, 1972) and the Balaisebut Group in Northwest Kalimantan (Zeijlmans van Emmichoven, 1939; Supriatna et al., 1993) (Fig. 1b). An equatorial position during the Mesozoic is also indicated for the overlying Jurassic Bau Limestone Formation (West Sarawak) and the equivalent Brandung Formation in NW Kalimantan (Beauvais & Fontaine, 1990; Schairer & Zeiss, 1992) (Fig. 1b).

A Cathaysian origin was consequently assumed for SW Borneo in the early syntheses (e.g. Metcalfe, 1990, 1994, 2006). In contrast, Hall et al. (2009) identified SW Borneo with the Banda block and suggested this continental fragment rifted from the Australian margin of

Gondwana in the Late Jurassic at c. 160 Ma (Hall et al., 2009; Hall, 2012), associated with Jurassic within-plate magmatism (Davies et al., 2014). Subduction and hinge retreat resulted in multiple phases of Cretaceous magmatism between c. 80 to 130 Ma during northward drifting of the SW Borneo block and widening of the Ceno-Tethys (Hall, 2012; Davies et al., 2014). According to this model, SW Borneo was accreted to the southeastern margin of Sundaland at around 110 Ma and subduction ceased at c. 90 Ma (Hall, 2012). Metcalfe (2009, 2011) followed the reconstruction of Hall et al. (2009) and accepted a Gondwana origin for SW Borneo.

Based on a fauna reported from the Terbat Limestone (Sanderson, 1966) and the Sadong Formation in West Sarawak, Metcalfe (1990, 2011) defined a Semitau terrane which was thought to have originated from Cathaysia and was accreted to Sundaland in the Cretaceous to Cenozoic. The existence of this terrane has been questioned by Breitfeld et al. (2017), who interpreted this area as part of the Triassic Sundaland margin and Mesozoic accretionary margin.

3. Field relations and petrography

The number of samples analysed in this study are relatively limited. This is owed to the fact that there is dense tropical rainforest vegetation and exposures of basement rocks are rare in the Pontianak area.

3.1 Meta-igneous rocks

The meta-igneous rocks in the research area are metamorphosed diorites, tonalites and granodiorites. Meta-diorite EK14-5 was sampled at a quarry west of Mount Tunggal (Fig. 2 and 3a). The steeply dipping rocks show a weak foliation and have been intruded by mafic and felsic dykes. Subsequent deformation resulted in the formation of small shear bands in the diorites and sheared folds in the dykes (Fig. 3b, c). Meta-diorites and mafic rocks are intruded by granitic rocks which are undeformed. All rocks are cut by brittle faults. The meta-diorites are composed of quartz, K-feldspar, plagioclase, amphibole, titanite and magnetite (Fig. 3d, e). Amphibole is abundant and aligned in a foliation. Irregular grain boundaries and grain size reduction indicate moderate dynamic recrystallisation.

Meta-granodiorite EK14-11 crops out in a tributary of the Pawan River southeast of Mount Biwa (Fig. 2 and 4a, b). It is composed of quartz, K-feldspar, plagioclase, biotite, titanite and magnetite. Biotite and magnetite are concentrated in foliation bands; biotite is partly altered to chlorite (Fig. 4c, d).

3.2 Granitoids and diorites

West Kalimantan

Undeformed granite EK14-1 was collected from the northwestern part of the study area at a quarry east of Pontianak (Fig. 2 and 5a). The rocks are composed of quartz, K-feldspar, plagioclase, biotite and subordinate white mica, and contain small mafic xenoliths and restites (c. 2-5 cm in length), indicating anatectic melting (Fig. 5b). Retrograde effects include local replacement of biotite by chlorite (Fig. 5c), and feldspar by sericite or (fibrous) epidote-group minerals (Fig. 5d). Undulose quartz, quartz subgrains, and grain boundary migration indicate minor deformation.

Sample EK14-6 is a coarse-grained undeformed tonalite (Fig. 6a) collected from float of the Kualan River northwest of Mount Tunggal (Fig. 2). It consists of quartz, K-feldspar phenocrysts, plagioclase, euhedral to subhedral amphibole, biotite, and accessory apatite and an opaque phase (Fig. 6b, c). Some quartz grains show irregular grain boundaries as a result of grain boundary migration due to minor dynamic recrystallisation. Locally, chlorite and epidote grew during retrograde metamorphism.

EK14-10 was sampled from an outcrop at a tributary of the Pawan River southeast of Mount Biwa (Fig. 2). The undeformed coarse-grained diorite is fractured and cut by felsic dykes of c. 4 cm thickness (Fig. 6d). It is composed of quartz, plagioclase, K-feldspar, biotite, clinopyroxene which is locally surrounded by amphibole, and an opaque phase (Fig. 6e, f).

West Sarawak

Sample TB76 and TB80 were collected from float of two nearby rivers in the Pueh range (Fig. 7a, b) where there is a large batholith west of Lundu at the western border of Sarawak with

Kalimantan (Fig. 1b). The coarse-grained undeformed granitoid TB76 contains mafic enclaves and is composed of quartz, plagioclase, K-feldspar, hypidiomorphic and xenomorphic biotite, amphibole and an opaque phase. Biotite is usually chloritized and feldspar partially altered to sericite. Another sample from this intrusive complex (TB80) has no amphibole, but abundant white mica, and contains small microgranular white mica - spinel - quartz - plagioclase enclaves (c. 0.2-1.0 cm in length) (Fig. 7c, d).

The Gading Intrusion is exposed east of the Pueh range near Lundu (Fig. 1b) and was sampled from an outcrop at Siar beach (TB69) and from float of a small river (TB71a). Sample TB71a is a two-mica granite which is cut by mafic/dioritic dykes and aplites, and is composed of quartz, plagioclase, K-feldspar, biotite and white mica. In contrast, sample TB69 contains abundant amphibole (Fig. 7e, f) and lacks white mica, resembling samples of the Pueh Intrusion.

4. Methodology

4.1 Bulk chemistry

Two metamorphic rocks and seven granitoids/diorites were analysed by whole-rock X-ray fluorescence (XRF) spectrometry at Royal Holloway University of London, UK (Tab. 1). Crushed rock chips were milled to a homogeneous powder in a TEMA disk mill using a tungsten carbide grinding barrel. Fusion disks (sample to spectroflux ratio of 1:6) and pressed pellets were prepared for analysis of major and trace element concentrations respectively using a PANalytical Axios sequential X-ray fluorescence spectrometer equipped with a 4 kW Rh-anode X-ray tube. Five standard analyses of the same granitoid sample were used for assessment of the reproducibility.

4.2 LA-ICP-MS

Zircons from samples analysed for bulk rock compositions were dated by U-Pb LA-ICP-MS at UCL/Birkbeck College, UK. Sample preparation was carried out at Royal Holloway University of London. The samples were crushed into small rock chips of c. 2 cm length in a jaw crusher, washed to avoid any contamination and subsequently dried in an oven. The chips

were further processed in a tungsten carbide disk mill and subsequently sieved through a 250 µm nylon tissue mesh to obtain a grain size fraction ≤250 µm. Heavy minerals were separated by using a Wilfley table or LST heavy liquid density separation (concentrated solution of lithium heteropolytungstates in water with a density between 2.89 and 2.96 g/cm^3), and zircons were separated using a Frantz isodynamic magnetic separator as well as DIM heavy liquid (di-iodomethane with a density of 3.3 g/cm^3) to purify the separates. The zircons were mounted in araldite resin and polished for exposure. Prior to analysis photomicrographs were obtained in transmitted light to identify cracks and inclusions, and cathodoluminescence (CL) imaging was performed on a Hitachi S3000N secondary electron microscope (SEM) at Royal Holloway University to identify internal structures used for analysis spot selection and data interpretation.

Analysis was carried out on a New Wave NWR 193 nm laser ablation system which is coupled to an Argilent 7700 quadrupole-based inductively-coupled plasma mass spectrometer (ICP-MS). It is operated with a two-cell sample chamber for background readings reduction and lower washout times. The Plešovice zircon (337.13 ± 0.37 Ma; Sláma et al., 2008) and NIST 612 silicate glass (Pearce et al., 1997) were used as standards. A beam size of c. 25 µm was used for analysis. Data reduction was performed using the GLITTER software package (Griffin et al., 2008) to process uncorrected U-Th-Pb isotope ratios and calculate ages with ±1σ errors. The ages obtained were corrected using the common Pb correction spreadsheet of Andersen (2002) which is proposed for a ^{204}Pb common Pb-independent analysis. Data analysed are presented in the Supplementary File 1. ^{206}Pb-^{238}U ages were compared to ^{207}Pb-^{235}U ages (for ages smaller than 1 Ga) or ^{207}Pb-^{206}Pb ages (for ages equal or greater than 1 Ga) and considered as discordant if the difference was greater than 10%.

Isoplot 4.11 (Ludwig, 2003) was used to create Concordia (Wetherill, 1956) and Tera-Wasserburg Concordia diagrams (Tera & Wasserburg, 1972). The youngest age population was determined using the unmix function of Sambridge & Compston (1994). Weighted mean ages were calculated for them (Supplementary File 2), excluding analyses which were interpreted to be affected by common Pb or Pb loss based on the Concordia and Tera-Wasserburg Concordia plots. Zircon age histograms and probability density plots were

311 calculated using an R script written by I. Sevastjanova based on the approach of Sircombe
312 (2004).
313

314 **5. Results**

315 **5.1 Geochemistry**

316 Analyses were acquired from fresh rocks. Thin sections presented in figures 3 to 7 show the
317 presence of fresh igneous minerals, such as feldspars, amphiboles or clinopyroxenes. There
318 is only minor alteration evident by some chlorite overgrowth in the granite EK14-1, and
319 therefore very little change in major element contents is likely. This is supported by low loss
320 on ignition (LOI) values between 0.34 and 0.97 wt % (Tab. 1). The two-mica granite TB71a
321 was the only sample with a higher LOI value of 2.71 wt % reflecting its high mica content.
322

323 Meta-igneous rocks may have experienced some metamorphic alteration. The SiO_2 vs. K_2O
324 diagram (Fig. 8) shows some variability in the K_2O contents for sample EK14-11 which plots
325 into the high-K calc-alkaline field. All other samples are calc-alkaline, forming a relatively
326 good linear correlation. Similar variations can be detected for the large ion lithophile
327 elements (especially for Rb) in the spider diagram (Fig. 8). However, the samples have
328 similar contents of immobile elements, suggesting systematic chemical changes are small.
329

330 Analyses were compared with those from metamorphic and magmatic samples reported
331 from West Sarawak (Kirk, 1968; Breitfeld et al., 2017) and the Schwaner Mountains in West
332 Kalimantan (Davies, 2013; Setiawan et al., 2013).
333

334 ***5.1.1 Meta-igneous rocks***

335 Four meta-igneous rocks from southeast of Pontianak (Fig. 2) were analysed and described
336 by Setiawan et al. (2013). They were classified as calc-alkaline metatonalites based on the
337 AFM diagram (Irvine & Baragar, 1971) and the CIPW normative An-Ab-Or diagram (Barker &
338 Arth, 1979). Negative Nb and Ti anomalies and positive Pb anomaly in the N-MORB
339 normalised spider diagram of Sun & McDonough (1989) indicate a subduction- and collision-
340 related tectonic setting (Setiawan et al., 2013). This is supported by volcanic arc granite

(VAG) signatures in the Rb vs. Yb + Ta geotectonic diagram of Pearce et al. (1984). Some of the metatonalites have relative high Sr/Y ratios and plot into the adakite field on the Sr/Y vs. Y diagram (Defant & Drummond, 1990) whereas all Cretaceous granitoids from the Schwaner Mountains analysed by Williams et al. (1988) have low Sr/Y ratios and fall into the Island Arc andesite-dacite-rhyolite field (Setiawan et al., 2013).

EK14-5 and EK14-11

EK14-5 plots into the (quartz-) diorite field in the TAS diagram of Cox et al. (1979), QAPF diagram (Streckeisen, 1974) as well as the R1-R2 plot of De La Roche et al. (1980) (Fig. 8a). The sample has a medium-K calc-alkaline composition in the SiO_2 vs K_2O diagram of Peccerillo & Taylor (1976) and is classified as a metaluminous I-type rock based on the ASI index of Frost et al. (2001) (Fig. 8b, c) and compositional discrimination criteria proposed by Chappell & White (1974, 2001), including an A/CNK index of 0.80, high CaO contents of 7.28 wt %, a CIPW normative diopside value of 8.52 and abundant amphibole and magnetite. Sample EK14-11 falls into the granodiorite fields in the TAS diagram and R1-R2 plot, has a high-K calc-alkaline composition, and plots at the transition of the metaluminous and peraluminous fields in the A/NK vs. ASI diagram (Fig. 8a-c). The rock has an I-type affinity based on an A/CNK index of 0.99, relatively high CaO contents of 3.54 wt %, a CIPW normative corundum value of 0.25 and abundant magnetite.

Both samples have similar high Fe-number indices of 0.75 and 0.78, relatively low MALI-indices of -1.65 and 3.03, and ASI indices of 0.8 and 0.99, classifying the rocks as magnesian, calcic, and metaluminous (to peraluminous) based on the discrimination diagrams of Frost et al. (2001). They are similar to the four samples of Setiawan et al. (2013), suggesting a similar tectonic origin and evolution for the meta-igneous samples.

Comparison to the Jagoi Granodiorite (West Sarawak)

Bulk rock compositions were presented for two samples of the Jagoi Granodiorite of West Sarawak by Kirk (1968) and Breitfeld et al. (2017).

Breitfeld et al. (2017) classified the Jagoi Granodiorite as a calc-alkaline metaluminous to peraluminous I-type granite according to the classification of Chappell & White (2001). The sample has very similar major and trace element compositions to the West Kalimantan samples, especially to EK14-11, and similar Fe-number of 0.77 and MALI index of 3.1. The Jagoi sample of Kirk (1968) plots close to the sample of Breitfeld et al. (2017) in the R1-R2, SiO_2 vs. K_2O and ASI diagrams but has a more peraluminous granitic composition, indicating a more evolved, crustal-influenced character (Fig. 8a-c). All analyses form a calc-alkaline magmatic trend (Fig. 8d) in the AFM diagram of Irvine & Baragar (1971). The sample of Kirk (1968) has the highest alkali content, indicating either crustal assimilation or fractionation within the group, possibly related to re-melting from multiple phases of magmatism.

Major and trace elements of all analyses were plotted on the N-MORB-normalised spider diagram (Sun & McDonough, 1989). All meta-igneous samples have similar negatively sloping trends showing enrichment in LILE and reduction of HFSE compared to the reference analyses (Fig. 8e). This pattern indicates a volcanic arc signature which supports a subduction-related origin. All analyses have negative Nb, La, Ce, P and Ti relative anomalies, and positive Pb anomalies. Three of the West Kalimantan analyses, including the meta-diorite EK14-5, show positive Ba and Sr anomalies and less prominent Rb and Th peaks which are due to a lesser crustal imprint. They plot at the less-fractionated, lower end of the magmatic suite (Fig. 8d). K, P and Ti were the only elements measured for the Jagoi Granodiorite sample of Kirk (1968) which is very similar to the Jagoi Granodiorite sample of Breitfeld et al. (2017).

5.1.2 Granitoids and diorites

West Kalimantan

Sample EK14-1 is a granite to granodiorite based on the TAS, QAPF and R1-R2 diagrams (Fig. 9a). It falls at the boundary of the medium- and high-K calc-alkaline fields in the SiO_2 vs. K_2O diagram (Fig. 9b) and is magnesian, calcic, and peraluminous (Frost et al., 2001) (Fig. 9c) with an S-type character based on high SiO_2 contents of 70.78 wt %, an A/CNK index of 1.07, a CIPW normative corundum value of 1.18, and the presence of white mica.

Sample EK14-6 is classified as a tonalite in the R1-R2 diagram or granodiorite in the QAPF diagram; sample EK14-10 is a diorite to quartz-monzodiorite according to the R1-R2 and QAPF diagrams (Fig. 9a). Both samples also plot at the boundary between the medium- and high-K calc-alkaline compositions in the SiO_2 vs. K_2O diagram but have significantly lower SiO_2 contents (c. 60-62 wt %) than sample EK14-1 (Fig. 9b). They are magnesian, calcic to calc-alkalic, and metaluminous (Fig. 9c) with I-type affinities as indicated by A/CNK values of 0.94 and 0.89, high CaO contents of 5.36 and 5.71, CIPW normative diopside values of 1.9 and 3.78, and abundant amphibole, clinopyroxene and magnetite.

All three samples have very similar negatively sloping patterns in the spider diagram of Sun & McDonough (1989). They show enriched concentrations of LILE with positive K and Pb peaks and negative Nb, La, Ce and Ti troughs, indicating arc-related magmas with a crustal component (Fig 9d). They also plot into the VAG field in the diagram of Pearce et al. (1984) (Fig 9e).

West Sarawak

The Pueh as well as the Gading Intrusions include rocks with I- and S-type characteristics according to the classification of Chappell & White (1974, 2001). Samples TB69 and TB76 have I-type and silica-rich/felsic I-type affinities respectively (A/CNK indices of 0.74 and 1.04; CaO contents of 6.19 and 2.81; CIPW normative diopside value of 8.7 and low corundum value of 0.71; abundant amphibole), whereas samples TB80 and TB71a are related to S-type chemistries (A/CNK indices of 1.19 and 1.61; CaO contents of 2.64 and 1.67; CIPW normative corundum values of 2.72 and 6.23; white mica present).

The felsic granite to granodiorite samples TB76, TB80 and TB71a are classified as high-K calc-alkaline (Peccerillo & Taylor, 1976) and magnesian, calc-alkaline to calcic, and peraluminous (Frost et al., 2001) (Fig. 9a-c). The mafic sample TB69 is a tonalite (R1-R2 plot) or granodiorite (QAPF diagram) and falls into the tholeiitic series in the AFM diagram but is classified as calc-alkaline in the SiO_2 vs. K_2O diagram (Fig. 9a, b). Although the felsic peraluminous samples show some scatter on most discrimination diagrams, they plot relatively close to one another. In contrast, sample TB69 often plots further away from

433 them and differs in its ferroan, calcic, and metaluminous character (Frost et al., 2001) (Fig.
434 9c).
435
436 All four samples plot close to the triple point of the VAG, WPG and syn-COLG fields in the
437 diagram of Pearce et al. (1984); samples TB76, TB80 and TB71a are volcanic arc granites,
438 and sample TB69 a within-plate granite (Fig. 9e), but according to Pearce (1996) all four
439 samples could also indicate a post-collisional (post-COLG) setting. The three felsic
440 peraluminous samples have very similar patterns on the spider diagram (Sun & McDonough,
441 1989) with an enrichment of LILE over HFSE, as well as a positive Pb peak and negative Nb
442 and Ti troughs, generally related to a crustal influenced arc-type setting (Fig. 9d). Sample
443 TB69 is the only sample which displays characteristics of within-plate granites with a
444 generally smoother pattern and enrichment in LILE as well as HFSE (Pearce, 1996).
445
446 *Comparison to the Cretaceous NSZ Sepauk Tonalites and Late Cretaceous SSZ within-plate*
447 *granite*
448 Davies (2013) and Davies et al. (2014) presented geochemical data and U-Pb zircon ages for
449 seven samples of the I-type granodiorites and tonalites of the NSZ and one alkali granite
450 from the SSZ which has a confirmed Late Cretaceous age based on U-Pb zircon analysis.
451
452 Samples EK14-6 and EK14-10 are very similar to the I-type NSZ magmatic rocks which are
453 gabbro-diorites, diorites and tonalites in the R1-R2 plot, calc-alkaline to high-K calc-alkaline
454 in the SiO_2 vs K_2O diagram and have magnesian, calcic to calc-alkalic, and metaluminous
455 chemistries (Fig. 9a-c) with arc magmatic characters in the tectonic diagram of Pearce et al.
456 (1984) and the N-MORB-normalised spider diagram of Sun & McDonough (1989) (Fig. 9d, e;
457 Davies, 2013; Davies et al., 2014). Sample EK14-1 has a peraluminous felsic composition
458 which has not been previously reported from the NSZ and differs from the mainly I-type
459 tonalitic rocks of this area (Fig. 9a-c) (Haile et al., 1977; Williams et al., 1988; Bladon et al.,
460 1989; Pieters & Sanyoto, 1993; Davies et al., 2014).
461
462 The high-K calc-alkaline rock from the SSZ was classified as a within-plate alkali-granite by
463 Davies et al. (2014) and interpreted as post-collisional. The sample is ferroan, has an A/NK

and ASI index close to 1 at the boundary to the peralkaline field (Frost et al., 2001), and falls well into the WPG field (Pearce et al., 1984) (Fig. 9a, c, e). The Upper Cretaceous Pueh and Gading Intrusions were also classified as post-collisional by Kirk (1968). The four samples analysed in this study have significant mineralogical and chemical variability. Comparison of the major and trace element concentrations in the N-MORB normalised spider diagram of Sun & McDonough (1989) shows similar curves for the Pueh and Gading Intrusions and the VAG rocks of this study, except for sample TB69 which has a smoother profile with enrichment of HFSE, suggesting within-plate characteristics (Fig. 9d). Most of the element concentrations differ from the SSZ alkali-granite which has more prominent relative peaks (Th, U, Pb, Y and Yb) and troughs (Ba, La, Ce, Sr, P and Ti). The Y vs. Sr/Y diagram of Defant & Drummond (1990) used for adakite discrimination shows some distinction between the VAG rocks and the post-collisional Pueh and Gading granitoids, which have very low Sr/Y ratios of <5 and generally higher Y values between c. 20 to 60 ppm (Fig. 9f), similar to the SSZ alkali granite of Davies et al. (2014).

5.2 U-Th-Pb zircon geochronology

5.2.1 Meta-igneous rocks

EK14-5

Sample EK14-5 was collected near to the Triassic metatonalite of Setiawan et al. (2013). The zircons separated are euhedral to subhedral and c. 140-450 μm in length. The internal morphology is dominated by oscillatory zoning, often with facetted centres, and some zircons show dark rims (Fig. 10a).

Fifty-seven concordant ages were acquired from 52 zircons which range between 211 ± 3 Ma and 248 ± 5 Ma. The majority of ages were obtained from oscillatory zoned zircons (213 ± 4 to 248 ± 5 Ma); nine ages were acquired from dark rims which yielded a similar to slightly younger age range between 211 ± 3 Ma and 237 ± 4 Ma. The probability density plot (Fig. 10a) shows a small younger population which has a weighted mean age of 213.0 ± 3.0 Ma (MSWD = 0.69; n = 5) and an older population which forms a dominant peak at 234.7 ± 1.3 Ma (MSWD = 1.16; n = 50). The latter is very similar to the age of 233 ± 3 Ma reported by Setiawan et al. (2013). Ages obtained from oscillatory zoned zircons indicate that

495 magmatism started in the Early Triassic and lasted until the Late Triassic. A small number of
496 zircons analysed show dark rims interpreted as metamorphic. They indicate metamorphism
497 during the Middle to Late Triassic. The youngest ages obtained of 211 ± 3 Ma from dark rims
498 suggest Late Triassic metamorphism which was contemporaneous with the youngest phase
499 of magmatism.
500
501 *EK14-11*
502 Meta-granodiorite EK14-11 was collected from the southeastern part of the study area (Fig.
503 2). Zircons are euhedral to subhedral and c. 90 to 375 µm in length. There are two different
504 types of zircons present. Most of the zircons are relatively small (c. 60 - 120 µm in length)
505 and contain dark inclusions as observed in CL images (Fig. 10b). Internal structures were
506 locally observed and show oscillatory zoning or convolute disturbed parts, indicating
507 magmatic and metamorphic origins. Three zircons were analysed which represent the
508 largest grain size fraction (c. 180-360 µm in length). They have a much brighter CL
509 reflectance than the small inclusion-rich zircons, and reveal patchy or homogeneous internal
510 structures (Fig. 10b), interpreted as metamorphic (Corfu et al., 2003).
511
512 Twenty-five concordant ages of 19 zircons were obtained from this sample. They yielded
513 one Ordovician age (450 ± 5 Ma) from an oscillatory zoned zircon, several Jurassic ages (147
514 ± 2 to 183 ± 2 Ma) from dark, inclusion-rich zircons, and subordinate Late Cretaceous ages
515 (86 ± 2 to 92 ± 3 Ma) from large, bright zircons (Fig. 10b). The probability density plot shows
516 three subpeaks for the Jurassic age population which have weighted mean ages of 149.8 ±
517 4.4 Ma (MSWD = 3.2; n = 5), 162.4 ± 1.8 Ma (MSWD = 0.58; n = 5) and 177.1 ± 2.9 Ma
518 (MSWD = 3.0; n = 8). They are interpreted to represent inheritance from multiple pulses of
519 magmatism and/or metamorphic recrystallisation. The Cretaceous ages are interpreted as
520 metamorphic based on the internal zircon morphology.
521

522 ***5.2.2 Granitoids and diorites***

523 *EK14-1*
524 The zircons are c. 80 to 250 µm in length with euhedral crystal shapes or subordinate
525 anhedral fragments. Most of the zircons are oscillatory zoned; some have bright oscillatory

zoned or homogeneous cores with a high CL reflectance, while others have dark inclusion-rich centres which are also mantled by oscillatory zoned rims with a lower CL reflectance (Fig. 11a).

The 57 concordant zircon ages acquired yielded one Carboniferous core age (346 ± 4 Ma), six Triassic ages (204 ± 3 to 231 ± 4 Ma) from oscillatory zoned or homogeneous cores, six Jurassic ages (161 ± 2 to 200 ± 2 Ma) from dark inclusion-rich cores or bright core and rim sites, and 44 Cretaceous ages (111 ± 2 to 138 ± 2 Ma) from oscillatory zoned zircons and rims (Fig. 11a). The latter show a wide age scatter that most likely represents several events. The youngest dominant peak of the Cretaceous ages gives a weighted mean age of 118.6 ± 1.1 Ma (MSWD = 4.9; n = 30) and is interpreted as the crystallisation age of the granite.

EK14-6

The zircons separated are euhedral to subhedral, c. 90 - 360 µm in length, and have predominantly oscillatory zoned internal structures (Fig. 11b). Fifty-eight concordant ages were obtained from 51 zircons. They yielded ages ranging between 96 ± 2 Ma and 118 ± 2 Ma and form a dominant age population in the probability density plot (Fig. 11b) with a weighted mean age of 101.5 ± 0.6 Ma (MSWD = 1.7; n = 53). This age is interpreted to represent a mid Cretaceous magmatic episode.

EK14-10

The zircons analysed are euhedral to subhedral and c. 90 - 360 µm in length. They are oscillatory zoned; some show homogeneous structures in the centre of the crystals which are mantled by oscillatory zoning, others show locally homogeneous overgrowth (Fig. 11c). Twenty-five concordant ages were acquired from 25 zircons which range from 76 ± 2 to 97 ± 1 Ma, forming a Late Cretaceous age population (Fig. 11c). The probability density plot indicates a dominant younger subpeak which has a weighted mean age of 81.1 ± 1.1 Ma and a small older subpeak at c. 96 Ma. The internal zircon morphologies are similar for both populations and indicate that the older ages reflect inheritance from an earlier pulse of magmatism, and were partly overprinted by a younger episode of Late Cretaceous magmatism.

TB76 – Pueh Intrusion

The sample contains zircon grains of c. 70 - 260 µm in length. All grains are euhedral and mainly prismatic. Oscillatory zoning is evident in most grains, often with sector zoning, and a few grains show patchy internal structures (Fig. 11d). Xenocrystic cores were rarely observed and are mantled by oscillatory zoned rims.

A total of 101 concordant U-Pb ages were obtained from 99 zircons. They include mainly Late Cretaceous ages and five inherited ages from xenocrystic cores and oscillatory zoned zircons which are Carboniferous (348 ± 3 Ma), Triassic (224 ± 2 Ma), Jurassic (177 ± 2 Ma) and Early Cretaceous (141 ± 2 Ma; 134 ± 2 Ma) (Fig. 11e). Late Cretaceous ages range from 73.0 ± 1.0 to 84.2 ± 0.9 Ma, (an age of 69.2 ± 2.0 Ma was considered to be affected by Pb loss and excluded). The probability density plot shows a unimodal distribution, indicating one dominant age population which has a weighted mean age of 78.6 ± 0.3 Ma (MSWD = 1.9; n = 78).

TB71a - Gading Intrusion

The zircons separated are between c. 130 - 210 µm in length, mainly euhedral to subhedral prismatic with a few elongate or subrounded grains, and show predominantly oscillatory zoning, or oscillatory or xenocrystic dark cores which are mantled by oscillatory zoned rims (Fig. 11e). A few zircons have patchy internal structures.

Forty-seven concordant ages were obtained from 51 zircons. Four zircons yielded Paleoproterozoic ages of c. 1.8 Ga (1782 ± 15 Ma; 1806 ± 22 Ma; 1833 ± 17 Ma) and 2562 ± 20 Ma which were analysed from dark cores (Fig. 11e). There are eight additional analyses from dark cores which yielded similar, however discordant, ages which also support these two inherited Paleoproterozoic age populations. Other inheritance obtained from dark cores are Neoproterozoic (754 ± 9 Ma) and Silurian (421 ± 5 Ma), and Permian-Triassic (231 ± 3 to 278 ± 5 Ma), Jurassic (162 ± 2 Ma; 177 ± 2 Ma) and Early Cretaceous (119 ± 2 to 125 ± 2 Ma) from oscillatory zoned and patchy zircons (Fig. 11e).

Inherited zircons are abundant and make up approximately half of all analyses acquired from this sample which is a common feature in S-type rocks (Williams et al., 1992). The

other half comprises zircons with Late Cretaceous ages ranging between 75 ± 3 Ma and 97 ± 1 Ma from mainly oscillatory zoned zircons and rims. They form a dominant age population in the probability density plot which has a weighted mean age of 79. 7 ± 1.0 Ma (MSWD = 3.3; n = 26), interpreted as crystallisation age, and two small older subpeaks at c. 91 Ma and 97 Ma obtained from dark cores. The Late Cretaceous zircon age distribution is very similar to sample EK14-10 from West Kalimantan which may suggest that this sample is also related to post-collisional magmatism.

6. Discussion

6.1 Early Mesozoic tectono-metamorphic history at the Sundaland margin

Early to Late Triassic and Jurassic zircons were dated in this study from two meta-igneous rocks as well as occurring as inherited grains in a Cretaceous granite from the northwestern part of the Schwaner Mountains. These ages are very different to those from widespread granitoids and metapelites of the Sepauk Tonalites and Pinoh Metamorphic Group of the NSZ which yielded almost entirely Cretaceous zircon U-Pb ages (Davies, 2013; Davies et al., 2014). Magmatism and volcanism, producing volcanogenic protoliths of the Pinoh metapelites, were interpreted as the product of subduction-related arc activity during northward drift of the SW Borneo block before accretion to Sundaland (Davies et al., 2014). The Triassic and Jurassic ages suggest that the study region in the northwest Schwaner Mountains was not part of the SW Borneo block and has a different tectonic history. We propose it represents the SE Sundaland Early Mesozoic active margin where arc diorites and granodiorites were later metamorphosed. The Kerait Schist and schists of the Tuang Formation (West Sarawak Metamorphics) south of Kuching have protoliths interpreted as volcaniclastic fore-arc sediments (Wilford & Kho, 1965; Tate & Hon, 1991; Breitfeld et al., 2017) with white mica $^{40}Ar/^{39}Ar$ cooling ages (Breitfeld et al., 2017), supporting a Triassic subduction-related tectonic setting.

Rocks of similar Triassic age were reported from the Embuoi Complex to the north in NW Kalimantan by Williams et al. (1988) and from the Jagoi Granodiorite in the western part of West Sarawak (Breitfeld et al., 2017), and were interpreted to define the southeastern margin of Sundaland in the Triassic (Hall & Breitfeld, in press; Breitfeld et al., 2017). The

results from this study confirm the presence of Triassic rocks further south in West Kalimantan (Setiawan et al., 2013) and also identify co-genetic Jurassic rocks which provide further information about the southeastern margin of Sundaland and its tectonic history.

Fig. 12 summarises the distribution of Lower Mesozoic rocks in West Borneo discussed earlier. The boundary to the east is well-defined by i) localised exposures of Cretaceous melanges to the east, e.g. Lubok Antu Melange, Boyan Melange, Kapuas Complex and Sejingkat Formation (Tan, 1979; Williams et al., 1988; Pieters et al., 1993; Tan, 1993; Hutchison, 2005; Breitfeld et al., 2017) and ii) abundant Cretaceous metapelites and igneous rocks in the NSZ to the east/southeast with no older rocks, as confirmed by U-Pb ages of detrital zircons from several modern river sands in the area (Davies, 2013; Davies et al., 2014). A small number of samples analysed from the SSZ by Davies (2013), van Hattum et al. (2013) and Davies et al. (2014) yielded weighted mean ages of c. 72-85 Ma which do not support a continuation of Triassic Sundaland to the south. The boundary proposed in Fig. 12 is considered as the minimum extent of Triassic Sundaland, because in the area shown with grey and yellow stripes there is limited data from the SSZ, and igneous rocks on the Karimata Islands are undated (they were inferred to be Upper Cretaceous based on correlation with the Sukadana Granite by Margono & Sanyoto, 1996). Triassic magmatic rocks reported from Belitung (e.g. Jones et al., 1977; Hamilton, 1979; Darbyshire, 1988) as well as a K-Ar age of c. 135 Ma obtained from a well c. 270 km southwest of Ketapang (Hamilton, 1979) provide some constraint on the southern margin. Subsequent faulting along the Lupar Line, a major strike-slip fault active during the latest Cretaceous and early Cenozoic (Hall, 2012; Breitfeld et al., 2017), is interpreted to offset the Sundaland-SW Borneo suture (Fig. 12).

6.2 Magmatic evolution of the region

Triassic

Triassic magmatism and metamorphism in the study area could be related to either northeast-directed Paleo-Tethys subduction from the west or west-directed Paleo-Pacific subduction from the east (Fig. 13a) based on the paleogeographic reconstructions of Holloway (1981, 1982), Taylor & Hayes (1983), Metcalfe (1999, 2000, 2011), Carter et al.

(2001), Carter & Clift (2008), Sevastjanova et al. (2016) and Breitfeld et al. (2017). A Paleo-Tethys interpretation would suggest that Triassic rocks of West Kalimantan are the southeastern continuation of the Malay-Thai Tin Belt (Hutchison, 1975; Metcalfe, 1988, 2000; Cobbing et al., 1986, 1992; Hutchison & Tan, 2009) which is subdivided into a Main Range Province and an Eastern Province (Bignell & Snelling, 1977; Cobbing et al., 1986; Krähenbuhl, 1991). High-precision ion microprobe zircon U-Pb ages presented by Searle et al. (2012) range from 198 ± 2 Ma to 219 ± 9 Ma in the western Main Range Province and 227 ± 2 Ma to 267 ± 2 Ma in the Eastern Province. However, as explained below, we favour a Paleo-Pacific interpretation.

Jurassic

The meta-granodiorite EK14-11 analysed in this study yielded Early to Late Jurassic zircons, indicating several pulses of magmatism at a relatively long-lived convergent margin. Jurassic subduction-related magmatism was also interpreted by Xu et al. (2016) from samples drilled in the South China Sea. This supports a Paleo-Pacific subduction origin since Jurassic magmatic rocks are not known in the Malay Peninsula (Fig. 13b). Their absence is explained by the closure of the Paleo-Tethys after collision of Sibumasu with Indochina-East Malaya (Metcalfe, 2011; Sevastjanova et al., 2011). A Paleo-Pacific subduction origin is also favoured by Breitfeld et al. (2017) for the Jagoi Granodiorite in West Sarawak based on its geographic position and provenance of nearby Triassic sediments (Sadong and Kuching Formations) which contain abundant detrital zircons dated at c. 1.8 Ga, indicating a derivation from the SE China margin (e.g. Yu et al., 2010; Xia et al., 2012; Liu et al., 2014). This supports earlier work of Pimm (1967) who compared the geochemistry of the Triassic Serian Volcanics in West Sarawak to rocks from the Malay Peninsula and concluded they belong to different volcanic suites of probably separate petrographic provinces. Thus, there is good evidence that Triassic and Jurassic rocks of West Borneo were formed at the Paleo-Pacific subduction zone.

Cretaceous

An S-type granodiorite (EK14-1) of c. 118 Ma age was analysed in this study. It contains abundant inherited zircons of Jurassic and Triassic age, consistent with partial melting of Sundaland margin meta-igneous basement rocks. The I-type tonalite EK14-6 and diorite

EK14-10 have mean ages of c. 100 and 81 Ma, respectively. They are very close to the meta-igneous rocks (Fig. 2) and we propose they formed at the Sundaland margin during Cretaceous magmatism related to Paleo-Pacific subduction (Fig. 13c). Other evidence for Early Cretaceous magmatism at the Sundaland margin includes inherited zircons (c. 119-141 Ma) from the Pueh and Gading granitoids in West Sarawak, as well as widespread Cretaceous granitoids (c. 118 to 87 Ma) in the Da Lat Zone of SE Vietnam (Nguyen et al., 2004; Shellnutt et al., 2013).

The magmatic rocks of West Kalimantan are geochemically very similar to diorites and tonalites reported further to the east in the NSZ which have similar Cretaceous ages ranging from c. 80 to 130 Ma (Davies, 2013; Davies et al., 2014). We suggest these Cretaceous subduction-related rocks in the NSZ did not form during northward drift of the SW Borneo block, but during subduction at the Paleo-Pacific margin after collision (Fig. 13c). This implies that the Banda/SW Borneo block arrived earlier in the Early Cretaceous than previously suggested, indicated by the onset of volcanic arc activity at c. 130 Ma.

The Jurassic and Cretaceous (meta-) igneous rocks possibly represent the source for Jurassic to Cretaceous zircons (c. 85-143 Ma) in the Pedawan Formation. Breitfeld et al. (2017) proposed the Schwaner Mountains as a source for these zircons, also consistent with an earlier arrival of the SW Borneo block.

Upper Cretaceous post-collisional magmatism

The Jurassic meta-granodiorite EK14-11 yielded a small number of concordant Cretaceous zircons of c. 86-92 Ma which are interpreted as metamorphic and may be related to the collision of the Argo/East Java-West Sulawesi (EJ-WS) block in the Late Cretaceous (Fig. 13d). Collision of this block coincided with termination of Paleo-Pacific subduction in Borneo and supports the suggestion that intrusions with ages of c. 80 Ma or younger could be post-collisional magmatism following accretion (Davies et al., 2014). Clements et al. (2011) suggested a termination of subduction in northern Borneo and the South China margin at c. 80 Ma.

The Pueh and Gading Intrusions were interpreted as post-collisional by Kirk (1968). Zircon U-Pb dating in this study yielded mean ages of c. 77 and 80 Ma respectively. Four samples analysed from the Pueh and Gading Intrusions have a large chemical composition variation which results in their classification from VAG to WPG, possibly reflecting the volcanic arc-signatures of the host rocks. Their post-collisional character is thus uncertain, but comparison to the within-plate alkali-granite from the SSZ, which has an age of c. 72 Ma, reveals some geochemical similarities and a within-plate character is favoured in this study.

The diorite EK14-10 with a c. 81 Ma mean age has mineralogical similarities to the post-collisional Gading Intrusion TB69, but it also shows strong geochemical similarities to the volcanic arc-related NSZ rocks reported by Davies (2013) and granodiorite and tonalite analysed in this study (EK14-1, EK14-6). The ages presented here can therefore be interpreted in two ways: (1) all Cretaceous intrusives younger than c. 85-90 Ma are products of post-collisional magmatism, or (2) subduction-related magmatism did not finish until c. 81 Ma when extensional within-plate magmatism began.

The Late Cretaceous Ankroet Complex in SE Vietnam also includes rocks of magnesian to ferroan chemistries and variable compositions from volcanic arc granites to within-plate granites which were also interpreted as possibly post-collisional (Shellnutt et al., 2013). Very little is known about their ages, but one sample of the Ankroet Complex was dated at c. 87 Ma (Shellnutt et al., 2013). Post-collisional magmatism in West Borneo and SE Vietnam indicates a widespread extensional phase following the termination of the Paleo-Pacific subduction (Fig. 13d).

7. Conclusions

Triassic and Jurassic meta-igneous rocks discovered in the NW Schwaner Mountains are very different from the almost entirely Cretaceous rocks in the northern Schwaner Mountains assigned to the SW Borneo block. The older Mesozoic rocks are similar in age and geochemistry to magmatic and metamorphic rocks described from the Kuching Zone in West Sarawak, supporting a continuation of the Early Mesozoic Sundaland margin further to the southeast than previously suggested.

The NW Schwaner Mountains were part of the Indochina-East Malaya block during the Mesozoic where there were episodes of magmatism and metamorphism at c. 238 Ma, 211 Ma, 177 Ma, 162 Ma and 150 Ma. These are interpreted as the result of Triassic and Jurassic Paleo-Pacific subduction which can be traced along the east Asian margin from Indochina into West Borneo.

Granitoids and diorites in the NW Schwaner Mountains include two I-type rocks with ages of c. 100 and 81 Ma and one S-type rock with an age of c. 118 Ma. These rocks, and similar rocks in North Schwaner Mountains, indicate a similar tectonic setting at the Paleo-Pacific subduction margin for SE Sundaland and the SW Borneo block from the Early Cretaceous (c. 130 Ma) onwards.

Subordinate Late Cretaceous metamorphic ages of c. 90 Ma from a Jurassic meta-igneous rock are possibly related to the collision of the Argo block with the Sundaland margin.

Probable post-collisional Pueh and Gading Intrusions in the northwest of West Sarawak have ages of c. 77 and 80 Ma. Post-collisional Upper Cretaceous granites are known from elsewhere in West Sarawak, from Central and NW Kalimantan, and similar rocks were reported from SE Vietnam. This post-collisional magmatism along the former Paleo-Pacific subduction margin from Indochina to SW Borneo indicates a widespread Late Cretaceous extensional phase.

Post-Mesozoic faulting along the Lupar Line probably influenced the present-day position of the boundary between Triassic Sundaland (West Borneo) and SW Borneo.

Acknowledgements

This study was supported by the SE Asia Research Group which is funded by a consortium of oil companies. We thank Nugroho Imam Setiawan for help with the planning of the fieldwork in West Kalimantan and identifying outcrop locations. Thomson Galin from the JMG (Minerals and Geoscience Department Malaysia, Sarawak) is acknowledged for help

and support during fieldwork in West Sarawak. Richard Mani Banda (JMG) and the EPU (Economic Planning Unit) and the SPU (State Planning Unit) of Malaysia gave permission to conduct fieldwork and sample in West Sarawak. Christina Manning and Matthew Thirlwall are thanked for carrying out the geochemical analysis and Martin Rittner (UCL/Birkbeck College) helped with the LA-ICP-MS analytical work. We would also like to thank local people in the areas of Pontianak and Kuching who helped as guides or boatmen during fieldwork. We appreciated the constructive feedback and comments by Chris Morley and an anonymous reviewer which improved the final version of the manuscript.

Figure captions:

Fig.1: Overview sketch maps of Borneo showing the location and geological zones of western Borneo. a) Outline of Borneo including the political divisions, and the geological zones defined by Haile (1974) for the West Kalimantan and West Sarawak regions. b) Detailed map of western Borneo showing the location of the research areas in West Kalimantan and West Sarawak, the main lithologies discussed in the text based on Heng (1992), Pieters & Sanyoto (1993) and Breitfeld et al. (2017), as well as the tectonic blocks based on Hall (2012), Hall & Sevastjanova (2012) and Breitfeld et al. (2017). G – Gading Intrusion, P – Pueh Intrusion, TD – Tanjong Datu Intrusion, TB – Tinteng Bedil Intrusion.

Fig. 2: Simplified geological map of the Schwaner Mountains in SW Borneo based on Pieters & Sanyoto (1993), including the sample locations from this study and reported in the literature that were used for geochemical comparisons.

Fig. 3: Field and thin section photographs of the meta-diorite EK14-5. a) Active quarry in the strongly fractured and steeply dipping rocks. b) Localised shear bands cutting the foliation. c) Mafic dykes and aplites which intruded the meta-diorite are also sheared and show evidence of deformation by cm-scale cuspate-lobate folds. d, e) Plane and crossed polarised photomicrographs showing amphibole-rich foliation bands and moderate dynamic recrystallisation by grain boundary migration and quartz subgrain formation.

Fig. 4: Field and thin section photographs of the meta-granodiorite EK14-11. a, b) Outcrop of foliated meta-granodiorites at a river. c, d) Plane and crossed polarised photomicrographs

showing mafic bands of biotite, opaque minerals and titanite and felsic bands of quartz and feldspar.

Fig. 5: Field and thin section photographs of the meta-granodiorite EK14-1. a) Outcrop of granitoid blocks in weathered matrix. b) The granites have small mafic restites, indicating anatectic melting. c, d) Two different photomicrographs in plane and crossed polarised light showing partial replacement of biotite by chlorite, and the presence of white mica.

Fig. 6: Field and thin section photographs of the tonalite EK14-6 (a-c) and diorite EK14-10 (d-f). a) Boulder of undeformed black and white speckled tonalite. b, c) Plane and crossed polarised photomicrographs showing large euhedral amphibole crystals. d) Outcrop of fractured undeformed diorite cut by an aplite. e, f) Plane and crossed polarised photomicrographs showing formation of retrograde amphibole rims around clinopyroxene.

Fig. 7: Field and thin section photographs of granitoids and diorites of the Pueh (a-d) and Gading (e, f) Intrusions in West Sarawak. a) View to the west to the Pueh Range forming a high mountain range in the western part of West Sarawak. b) Large boulders in float of a small river draining the Pueh Range. c, d) Plane and crossed polarised photomicrographs of a felsic Pueh granitoid (TB80) showing the contact of a fine-grained spinel - white mica enclave (right side) to coarse-grained quartz and feldspar crystals of the granitoid (left side). e, f) Plane and crossed polarised photomicrographs of a mafic Gading intrusion (TB69) with abundant amphibole.

Fig. 8: Geochemical discrimination diagrams for the meta-igneous rocks analysed in this study and reported for West Kalimantan and West Sarawak by Kirk (1968), Setiawan et al. (2013) and Breitfeld et al. (2017). a) The rocks are classified as gabbro-diorites to granites in the R1-R2 diagram of De La Roche et al. (1980), with b) calc-alkaline to subordinately high-K calc-alkaline (Peccerillo & Taylor, 1976), and c) metaluminous to peraluminous chemistries (Frost et al., 2001). d) All rocks discussed form a calc-alkaline trend of a magmatic suite in the AFM diagram (Irvine & Baragar, 1971). e) N-MORB normalised spider diagram of Sun & McDonough (1989) showing similar volcanic-arc signatures for all meta-igneous rocks of West Kalimantan and West Sarawak.

Fig. 9: Geochemical discrimination diagrams for the granitoids and diorites of West Kalimantan and West Sarawak analysed in this study and data from the literature reported by Davies (2013) which is used for comparison. The rocks analysed from the NW Schwaner Zone are similar to the rocks of the NSZ (Davies, 2013) in the a) R1-R2 diagram (De La Roche et al. (1980), b) the SiO_2 vs K_2O diagram (Peccerillo & Taylor, 1976), c) the discrimination diagrams of Frost et al. (2001), d) the N-MORB normalised spider diagram of Sun & McDonough (1989) as well as e) the geotectonic discrimination diagram (Pearce et al., 1984) and f) the adakite diagram (Defant & Drummond, 1990) due to a similar origin from a volcanic-arc setting. The post-collisional Pueh and Gading rocks analysed from West Sarawak are very variable but show some similarities to the post-collisional alkali granite from the SSZ of Davies (2013).

Fig. 10: U-Pb zircon data from the meta-igneous rocks EK14-5 (a) and EK14-11 (b) of West Kalimantan, showing age histograms with probability density plots, age populations using the unmix function in Isoplot (Ludwig, 2003), Tera-Wasserburg Concordia diagrams (black circles – concordant; red circles – discordant) and CL images with selected analysis spots and ages obtained. The spot size was c. 25 µm; spot numbers are listed in the data tables in the Supplementary File 1.

Fig. 11: U-Pb zircon data from the granitoids and diorites of West Kalimantan: a) EK14-1, b) EK14-6, c) EK14-10, and West Sarawak: d) TB76, e) TB71a, showing age histograms with probability density plots, Tera-Wasserburg Concordia diagrams (black circles – concordant; red circles – discordant) and CL images with selected analysis spots and ages obtained. The spot size was c. 25 µm; spot numbers are listed in the data tables in the Supplementary File 1.

Fig. 12: Modified tectonic block diagram after Hall (2012), Hall & Sevastjanova (2012) and Breitfeld et al. (2017) showing the southeastern extent of Triassic Sundaland into the NW Schwaner Zone and possibly further south, previously assigned to the SW Borneo block. The distinction is based on abundant Early Mesozoic magmatic and metamorphic rocks in West Borneo, summarised from this study and literature data (Jones et al., 1977; Darbyshire,

1988; Williams et al., 1988; Breitfeld et al., 2017) that contrast with Cretaceous melange to the east (Tan, 1979; Williams et al., 1988; Pieters et al., 1993; Tan, 1993; Hutchison, 2005; Breitfeld et al., 2017) and Cretaceous magmatic and metamorphic rocks exposed further to the southeast and south with no older rocks (Hamilton, 1979; Davies, 2013; van Hattum et al., 2013; Davies et al., 2014). The ages shown are mean ages or age ranges of inherited detrital zircons obtained by zircon U-Pb analysis except where indicated otherwise.

Fig. 13: Paleogeographic reconstructions, modified from Metcalfe (2011), Hall (2012), Hennig et al. (2016), Sevastjanova et al. (2016) and Breitfeld et al. (2017), showing a) Meso-Tethys and Paleo-Pacific subduction in the Late Triassic (Paleo-Tethys subduction ceased after the collision of Sibumasu with Indochina), b) continuous Paleo-Pacific subduction and northward drift of the Banda, Argo and Inner Banda (IB) blocks, c) Accretion of the Banda block (SWB) to Sundaland and Early Cretaceous magmatism in West Borneo and SW Borneo (Banda block), d) Accretion of the Argo (East Java-West Sulawesi) and Inner Banda (NW Sulawesi/ Sabah) blocks followed by termination of the Paleo-Pacific subduction and post-collisional magmatism along the former active continental margin due to extension.

Table caption:

Tab. 1: Whole-rock major and trace element X-ray fluorescence data for samples from West Kalimantan and West Sarawak.

References

Amiruddin, Trail, D.S., 1993. Geology of the Nangapinoh Sheet area, Kalimantan, Geological Research and Development Centre, Bandung, 49 pp.

Andersen, T., 2002. Correction of common lead in U–Pb analyses that do not report 204 Pb. Chemical Geology 192 (1), 59-79.

Barker, F., Arth, J.G., 1979. Trondhjemite: definition, environment and hypotheses or orgin. In: Barker, F. (Ed.), Trondhjemites, dacites, and related rocks. Elsevier, New York, pp. 1– 12.

Basir J., Uyop S., 1999. Significance of Early Jurassic Radiolaria from West Sarawak, Malaysia. GEOSEA '98 Proceedings, Bulletin of the Geological Society of Malaysia 43, 491-502.

Bayliss, D.D., 1966. Foraminifera from the Bau Limestone Formation, Sarawak, Malaysia. Malaysia Geological Survey Borneo Region, Annual Report for 1965, 173-175.

Beauvais, L., Fontaine, H., 1990. Corals from the Bau Limestone Formation, Jurassic of Sarawak, Malaysia. In: Fontaine, H. (Ed.), Ten years of CCOP research on the Pre-Tertiary of east Asia, 209-239.

Ben-Avraham, Z., Uyeda S., 1973. The evolution of the China Basin and the Mesozoic palaeogeography of Borneo. Earth and Planetary Science Letters 18, 365-376.

Bignell, J.D., Snelling, N.J., 1977. Geochronology of Malayan granites. Overseas Geology and Mineral Resources 47. Institute of Geological Sciences, H.M. Stationary Office, London, 72 pp.

Bladon, G.M., Pieters, P.E., Supriatna, S., 1989. Catalogue of isotopic ages commissioned by the Indonesia-Australia Geological Mapping Project for igneous and metamorphic rocks in Kalimantan, Preliminary Report. Geological Research and Development Centre, Bandung.

Breitfeld, H.T., Hall, R., Galin, T., Forster, M.A., BouDagher-Fadel, M.K., 2017. A Triassic to Cretaceous Sundaland-Pacific subduction margin in West Sarawak, Borneo. Tectonophysics 694, 35-56.

Carter, A., Clift, P.D., 2008. Was the Indosinian orogeny a Triassic mountain building or a thermotectonic reactivation event? Comptes Rendus Geoscience 340 (2), 83-93.

Carter, A., Roques, D., Bristow, C., Kinny, P., 2001. Understanding Mesozoic accretion in Southeast Asia: significance of Triassic thermotectonism (Indosinian orogeny) in Vietnam. Geology 29 (3), 211-214.

Chappell, B.W., White, A.J.R., 1974. Two contrasting granite types. Pacific geology 8 (2), 173-174.

Chappell, B.W., White, A.J.R., 2001. Two contrasting granite types: 25 years later. Australian Journal of Earth Sciences 48 (4), 489-499.

Clements, B., Burgess, P.M., Hall, R., Cottam, M.A., 2011. Subsidence and uplift by slab-related mantle dynamics: a driving mechanism for the Late Cretaceous and Cenozoic evolution of continental SE Asia? In: Hall, R., Cottam, M.A., Wilson, M.E.J. (Eds.), The SE Asian Gateway: History and Tectonics of the Australia – Asia Collision. Geological Society, London, Special Publications 355, 37-51.

Cobbing, E.J., Mallick, D.I.J., Pitfiled, P.E.J., Teoh, L.H., 1986. The granites of the Southeast Asian Tin Belt. Journal of the Geological Society of London 143, 537–550.

Cobbing, E.J., Pitfield, P.E.J., Derbyshire, D.P.F., Mallick, D.I.J., 1992. The Granites of the South-East Asian Tin Belt. Overseas Memoirs 10, British Geological Survey.

Corfu, F., Hanchar, J.M., Hoskin, P.W.O., Kinny, P.D., 2003. Atlas of zircon textures. Reviews in Mineralogy and Geochemistry 53 (1), 469–500.

Cox, K.G., Bell, J.D., Pankhurst, R.J., 1979. The interpretation of igneous rocks. George Allen and Unwin, London.

Darbyshire, D.P.F., 1988. South-east Asia granite project: Geochronology of Tin Islands granites, Indonesia: Nat. Environment Research Council [U.K.] Isotope Geology Rept. 88/4, 1-16.

Davies, L.B., 2013. SW Borneo Basement: Age, origin and character of igneous and metamorphic rocks from the Schwaner Mountains, Royal Holloway University of London**,** 391 pp.

Davies, L., Hall, R., Armstrong, R., 2014. Cretaceous crust in SW Borneo: petrological, geochemical and geochronological constraints from the Schwaner Mountains. Proceedings Indonesian Petroleum Association, 38th Annual Convention and Exhibition, IPA14-G-025.

Defant, M.J., Drummond, M.S., 1990. Derivation of some modern arc magmas by melting of young subducted lithosphere. Nature 347 (6294), 662-665.

De Keyser, F., Rustandi, E., 1993. Geology of the Ketapang Sheet area, Kalimantan, 1:250,000. Geological Research and Development Centre, Bandung.

De La Roche, H., Leterrier, J.T., Grandclaude, P., Marchal, M., 1980. A classification of volcanic and plutonic rocks using R_1R_2-diagrams and major-element analyses - Its relationships with current nomenclature. Chemical Geology 29 (1-4), 183-210.

Frost, B.R., Barnes, C.G., Collins, W.J., Arculus, R.J., Ellis, D.J., Frost, C.D., 2001. A Geochemical Classification for Granitic Rocks. Journal of Petrology 42 (11), 2033-2048.

Griffin, W.L., Powell, W.J., Pearson, N.J., O'Reilly, S.Y., 2008. GLITTER: data reduction software for laser ablation ICP-MS. Laser Ablation-ICP-MS in the earth sciences. Mineralogical association of Canada short course series 40, 204-207.

Haile, N.S., 1974. Borneo. In: Spencer, A.M. (Ed.), Mesozoic-Cenozoic Orogenic Belts. Geological Society of London Special Publications 4, 333-347.

Haile, N.S., McElhinny, M.W., McDougall, I., 1977. Palaeomagnetic data and radiometric ages from the Cretaceous of West Kalimantan (Borneo), and their significance in interpreting regional structure. Journal of the Geological Society of London 133, 133-144.

Hall, R., 2012. Late Jurassic–Cenozoic reconstructions of the Indonesian region and the Indian Ocean. Tectonophysics 570, 1-41.

Hall, R., Sevastjanova, I., 2012. Australian crust in Indonesia. Australian Journal of Earth Sciences 59 (6), 827-844.

Hall, R., Breitfeld, H.T., 2017. Nature and Demise of the Proto-South China Sea, Bulletin of the Geological Society of Malaysia 63 (in press).

Hall, R., Clements, B., Smyth, H.R., 2009. Sundaland: Basement character, structure and plate tectonic development. Proceedings Indonesian Petroleum Association, 33rd Annual Convention.

Hamilton, W., 1979. Tectonics of the Indonesian region. U. S. Geological Survey Professional Paper 1078, 345 pp.

Heng, Y.E., 1992. Geological map of Sarawak, 1:500,000. Geological Survey of Malaysia.

Hennig, J., Hall, R., Armstrong, R.A., 2016. U-Pb zircon geochronology of rocks from west Central Sulawesi, Indonesia: Extension-related metamorphism and magmatism during the early stages of mountain building. Gondwana Research 32, 41-63.

Heryanto, R., Jones, B.G., 1996. Tectonic development of Melawi and Ketungau Basins, Western Kalimantan, Indonesia. Bulletin Geological Research and Development Centre, Bandung 19, 151-179.

Holloway, N.H., 1981. The North Palawan block, Philippines: its relation to the Asian mainland and its role in the evolution of the South China Sea. Bulletin of the Geological Society of Malaysia 14, 19-58.

Holloway, N.H., 1982. North Palawan block – its relation to Asian mainland and role in evolution of South China Sea. American Association of Petroleum Geologists Bulletin 66, 1355-1383.

Hutchison, C.S., 1975. Ophiolite in Southeast Asia. Geological Society of America Bulletin 86, 797-806.

Hutchison, C.S., 2005. Geology of North-West Borneo. Sarawak, Brunei and Sabah. Elsevier, Amsterdam, Netherlands, 421 pp.

Hutchison, C.S., Tan, D.N.K. (Eds.), 2009. Geology of Peninsular Malaysia. University of Malaya.

Irvine, T.N., Baragar, W.R.A., 1971. A guide to the chemical classification of the common volcanic rocks. Canadian journal of earth sciences 8 (5), 523-548.

JICA, 1985. Report on the collaborative mineral exploration of the Bau area, west Sarawak. Published report, BMG (March), 97 pp.

Jones, M.T., Reed, B.L., Doe, B.R., Lanphere, M.A., 1977. Age of tin mineralization and plumbotectonics, Belitung, Indonesia. Economic Geology 72 (5), 745-752.

Kirk, H.J.C., 1968. The igneous rocks of Sarawak and Sabah. Geological Survey, Borneo Region, Malaysia, Bulletin 5, 210 pp.

Kon'no, E., 1972. Some Late Triassic plants from the southwestern border of Sarawak, East Malaysia. Geology and Palaeontology of Southeast Asia (University of Tokyo Press) 10, 125-178.

Krähenbuhl, R., 1991. Magmatism, tin mineralization and tectonics of the Main Range, Malaysian Peninsula: consequences for the plate tectonic model of Southeast Asia based on Rb–Sr, K–Ar and fission track data. Bulletin of the Geological Society of Malaysia 29, 1–100.

Longley, I.M., Buessenschuett, C., Clydsdale, L., Cubitt, C.J., Davis, R.C., Johnson, M.K., Marshall, N.M., Murr, A.P., 2002. The North West Shelf of Australia - a Woodside perspective. In: Keep, M., Moss, S.J. (Eds.), The Sedimentary Basins of Western Australia III, Proceedings West Australian Basins Symposium, Perth 2002. Petroleum Exploration Society of Australia, 28-86.

Liu, L., Xu, X. S., Xia, Y., 2014. Cretaceous Pacific plate movement beneath SE China: evidence from episodic volcanism and related intrusions. Tectonophysics 614, 170-184.

Ludwig, K.R., 2003. User's Manual for Isoplot 3.0: A Geochronological Toolkit for Microsoft Excel. Berkeley Geochronology Center Special Publication 4, 71 pp.

Margono, U., Sanyoto, P., 1996. Geological map of the Karimata (Tanjungpasir) Quadrangle, Kalimantan. Map at 1:250000 scale. Geological Research and Development Centre, Bandung.

Metcalfe, I., 1988. Origin and assembly of South-East Asian continental terranes. In: Audley-Charles, M.G., Hallam, A. (Eds.), Gondwana and Tethys. Geological Society of London Special Publication 37, 101–118.

Metcalfe, I., 1990. Allochthonous terrane processes in Southeast Asia. Philosophical Transactions. Royal Society of London A331, 625–640.

Metcalfe, I., 1994. Gondwanaland origin, dispersion, and accretion of East and Southeast Asian continental terranes. Journal of South American Earth Sciences *7* (3-4), 333-347.

Metcalfe, I., 1999. The Palaeo-Tethys in East Asia. GEOSEA '98 Bulletin of the Geological Society of Malaysia 43, 131-143.

Metcalfe, I., 2000. The Bentong–Raub Suture Zone. Journal of Asian Earth Sciences 18, 691–712.

Metcalfe, I., 2006. Palaeozoic and Mesozoic tectonic evolution and palaeogeography of East Asian crustal fragments: The Korean Peninsula in context. Gondwana Research 9, 24-46.

Metcalfe, I., 2009. Late Palaeozoic and Mesozoic tectonic and palaeogeographical evolution of SE Asia. In: Buffetaut, G., Cuny, Le Loeuff, J., Suteethorn, V. (Eds.), Late Palaeozoic and Mesozoic Ecosystems in SE Asia. Geological Society of London Special Publication 315, 7-23.

Metcalfe, I., 2011. Palaeozoic-Mesozoic history of SE Asia. In: Hall, R., Cottam, M.A., Wilson, M.E.J. (Eds.), The SE Asian Gateway: History and Tectonics of the Australia-Asia Collision. Geological Society, London, Special Publication 355, 7–35.

Morley, R.J., 1998. Palynological evidence for Tertiary plant dispersals in the SE Asian region in relation to plate tectonics and climate. In Hall, R., Holloway, J. D. (Eds.), Biogeography and Geological Evolution of SE Asia. Backhuys Publishers, Leiden, The Netherlands, 211-234.

Muller, J., 1968. Palynology of the Pedawan and Plateau Sandstone Formations (Cretaceous - Eocene) in Sarawak, Malaysia. Micropaleontology 14, 1-37.

Nguyen, T.T.B., Satir, M., Siebel, W., Chen, F., 2004. Granitoids in the Dalat zone, southern Vietnam: age constraints on magmatism and regional geological implications. International Journal of Earth Sciences 93, 329–340.

Nuraiteng, T.A., Kushairi, H., 1987. Pedawan Formation of the Penrissen Area, Sarawak: A revision of its upper age limit. Warta Geologi, Geological Society of Malaysia Newsletter 13 (2), 43-50.

Pearce, J., 1996. Sources and settings of granitic rocks. Episodes 19, 120-125.

Pearce, J.A., Harris, N.B.W., Tindle, A.G., 1984. Trace element discrimination diagrams for the tectonic interpretation of granitic rocks. Journal of Petrology 25 (4), 956-983.

Pearce, N.J.G., Perkins, W.T., Westgate, J.A., Gorton, M.P., Jackson, S.E., Neal, C.R., Chenery, S.P., 1997. A Compilation of New and Published Major and Trace Element Data for NIST SRM 610 and NIST SRM 612 Glass Reference Materials. Geostandards Newsletter 21 (1), 115-144.

Peccerillo, A., Taylor, S.R., 1976. Geochemistry of Eocene calc-alkaline volcanic rocks from the Kastamonu area, northern Turkey. Contributions to Mineralogy and Petrology 58 (1), 63-81.

Pieters, P.E., Sanyoto, 1993. Geological map of the Pontianak/Nangataman Sheet, Kalimantan. Map at 1:250000 scale. Geological Research and Development Centre, Bandung.

Pieters, P.E., Surono, Noya, Y., 1993. Geology of the Putussibau Sheet area, Kalimantan. Geological Survey of Indonesia, Directorate of Mineral Resources, Geological Research and Development Centre, Bandung, Quadrangle 1616, 1:250000.

Pimm, A.C., 1965. Serian area, west Sarawak, Malaysia. Geological Survey of Malaysia, Borneo Region 3, 92 pp.

Pimm, A.C., 1967. Triassic volcanic rocks in East and West Malaysia. In: Collenette, P. (Ed.), Geological Papers 1966, Bulletin 8. Geological Survey Borneo Region Malaysia, Kuching, pp. 36-40.

Sambridge, M.S., Compston, W., 1994. Mixture modeling of multi-component data sets with application to ion-probe zircon ages. Earth and Planetary Science Letters 128, 373–390.

Sanderson, G.A., 1966. Presence of Carboniferous in West Sarawak: Geological Notes. American Association of Petroleum Geologists Bulletin 50, 578-580.

Schairer, G., Zeiss, A., 1992. First record of Callovian ammonites from West Kalimantan (Middle Jurassic, Kalimantan Barat, Borneo, Indonesia). BMR Journal of Australian Geology and Geophysics 13 (3), 229-236.

Searle, M.P., Whitehouse, M.J., Robb, L.J., Ghani, A.A., Hutchison, C.S., Sone, M., Ng, S.W.-P., Roselee, M.H., Chung, S.-L., Oliver, G.J.H., 2012. Tectonic evolution of the Sibumasu–Indochina terrane collision zone in Thailand and Malaysia: constraints from new U-Pb zircon chronology of SE Asian tin granitoids. Journal of the Geological Society, London 169, 89–500.

Setiawan, N.I., Osanai, Y., Nakano, N., Adachi, T., Setiadji, L.D., Wahyudiono, J., 2013. Late Triassic metatonalite from the Schwaner Mountains in West Kalimantan and its contribution to sedimentary provenance in the Sundaland. Berita Sedimentologi 12, 4-12.

Sevastjanova, I., Clements, B., Hall, R., Belousova, E.A., Griffin, W.L., Pearson, N., 2011. Granitic magmatism, basement ages, and provenance indicators in the Malay Peninsula: Insights from detrital zircon U-Pb and Hf-isotope data. Gondwana Research 19 (4), 1024-1039.

Sevastjanova, I., Hall, R., Rittner, M., Paw, S.M.T.L., Naing, T.T., Alderton, D.H., Comfort, G., 2016. Myanmar and Asia united, Australia left behind long ago. Gondwana Research 32, 24-40.

Shellnutt, J.G., Lan, C.Y., Van Long, T., Usuki, T., Yang, H.J., Mertzman, S.A., Hsu, W.Y., 2013. Formation of Cretaceous Cordilleran and post-orogenic granites and their microgranular

enclaves from the Dalat zone, southern Vietnam: Tectonic implications for the evolution of Southeast Asia. Lithos 182, 229-241.

Sircombe, K.N., 2004. AgeDisplay: an EXCEL workbook to evaluate and display univariate geochronological data using binned frequency histograms and probability density distributions. Computers Geosciences 30, 21-31.

Sláma, J., Košler, J., Condon, D.J., 2008. Plešovice zircon - A new natural reference material for U–Pb and Hf isotopic microanalysis. Chemical Geology 249 (1–2), 1-35.

Streckeisen, A., 1974. Classification and nomenclature of plutonic rocks recommendations of the IUGS subcommission on the systematics of Igneous Rocks. Geologische Rundschau 63, 773-786.

Sun, S.S., McDonough, W., 1989. Chemical and isotopic systematics of oceanic basalts: implications for mantle composition and processes. Geological Society of London Special Publications 42, 313-345.

Supriatna, S., Margono, U., Sutrisno, de Keyser, F., Langford, R.P., Trail, D.S., 1993. Geology of the Sanggau sheet area, Kalimantan. Geological Survey of Indonesia, Directorate of Mineral Resources, Geological Research and Development Centre, Bandung, 1:250000.

Tan, D.N.K., 1979. Lupar Valley, west Sarawak. Geological Survey of Malaysia, Report 13.

Tan, D.N.K., 1993. Geology of the Kuching area. West Sarawak, Malaysia. Geological Survey of Malaysia, Report 16.

Tate, R.B., 1991. Cross-border correlation of geological formations in Sarawak and Kalimantan. Bulletin of the Geological Society of Malaysia 28, 63-96.

Tate, R.B., Hon, V., 1991. The oldest rocks in Borneo; a note on the Tuang Formation, West Sarawak and its importance in relation to the presence of a ”basement” in West Borneo. Warta Geologi, Geological Society of Malaysia Newsletter 17, 221-224.

Taylor, B., Hayes, D.E., 1983. Origin and history of the South China Sea basin. In: Hayes, D.E. (Ed.), The Tectonic and Geologic Evolution of Southeast Asian Seas and Islands, Part 2. American Geophysical Union, Geophysical Monographs Series 27, 23-56.

Tera, F., Wasserburg, G.J., 1972. U-Th-Pb systematics in three Apollo 14 basalts and the problem of initial Pb in lunar rocks. Earth and Planetary Science Letters 14 (3), 281-304.

Ting, C.S., 1992. Jurassic-Cretaceous palaeogeography of the Jagoi-Serikin area as indicated by the Bau Limestone Formation. Bulletin of the Geological Society of Malaysia 31, 21-38.

van Bemmelen, R.W., 1949 (2nd edition 1970). The Geology of Indonesia. (3 Vols) Vol. 1a: General Geology of Indonesia and Adjacent Archipelagos. Vol.1b: Portfolio (maps, charts,

indexes and references). Vol.2: Economic Geology. Govt. Printing Office, Nijhoff, The Hague (2nd edition, 1970), 732 pp.

van Hattum, M.W.A., Hall, R., Pickard, A.L., Nichols, G.J., 2013. Provenance and geochronology of Cenozoic sandstones of northern Borneo. Journal of Asian Earth Sciences 76, 266-282.

Wetherill, G.W., 1956. Discordant uranium-lead ages. Transactions, American Geophysical Union 37, 320-326.

Wilford, G.E., Kho, C.H., 1965. Penrissen area, west Sarawak, Malaysia. Geological Survey, Borneo Region, Malaysia, Report 2.

Williams, P.R., Johnston, C.R., Almond, R.A., Simamora, W.H., 1988. Late Cretaceous to Early Tertiary structural elements of West Kalimantan. Tectonophysics 148 (3/4), 279-298.

Williams, I.S., Chappell, B.W., Chen, Y.D., Crook, K.A.W., 1992. Inherited and detrital zircons—vital clues to the granite protoliths and early igneous history of southeastern Australia. Transactions of the Royal Society of Edinburgh: Earth Sciences 83, 503 pp.

Wolfenden, E.B., 1965. Bau Mining District, West Sarawak, Malaysia, part I. Bau. Geological Survey, Borneo Region, Malaysia, Bulletin 7, 147 pp.

Xia, Y., Xu, X.S., Zhu, K.Y., 2012. Paleoproterozoic S- and A-type granites in southwestern Zhejiang: magmatism, metamorphism and implications for the crustal evolution of the Cathaysia basement. Precambrian Research 216-219, 177–207.

Xu, C., Shi, H., Barnes, C.G., Zhou, Z., 2016. Tracing a late Mesozoic magmatic arc along the Southeast Asian margin from the granitoids drilled from the northern South China Sea. International Geology Review 58 (1), 71-94.

Yanagida, J., Lau, M., 1978. The Upper Jurassic and Middle Cretaceous Terebratulidae from the Bau Limestone Formation in West Sarawak, Malaysia. Geology and Palaeontology of Southeast Asia (University of Tokyo Press) 19, 35-47.

Yu, J.H., O'Reilly, S.Y., Wang, L.J., Griffin, W.L., Zhou, M.F., Zhang, M., Shu, L.S., 2010. Components and episodic growth of Precambrian crust in the Cathaysia Block, South China: evidence from U-Pb ages and Hf isotopes of zircons in Neoproterozoic sediments. Precambrian Research 181, 97–114.

Zeijlmans van Emmichoven, C.P.A., 1939. De geologie van het centrale en oostelijke deel van de Westerafdeeling van Borneo. Jaarboek Mijnwezen Nederlandsch Oost Indië, Verhandelingen 1939, 68, 7-186.

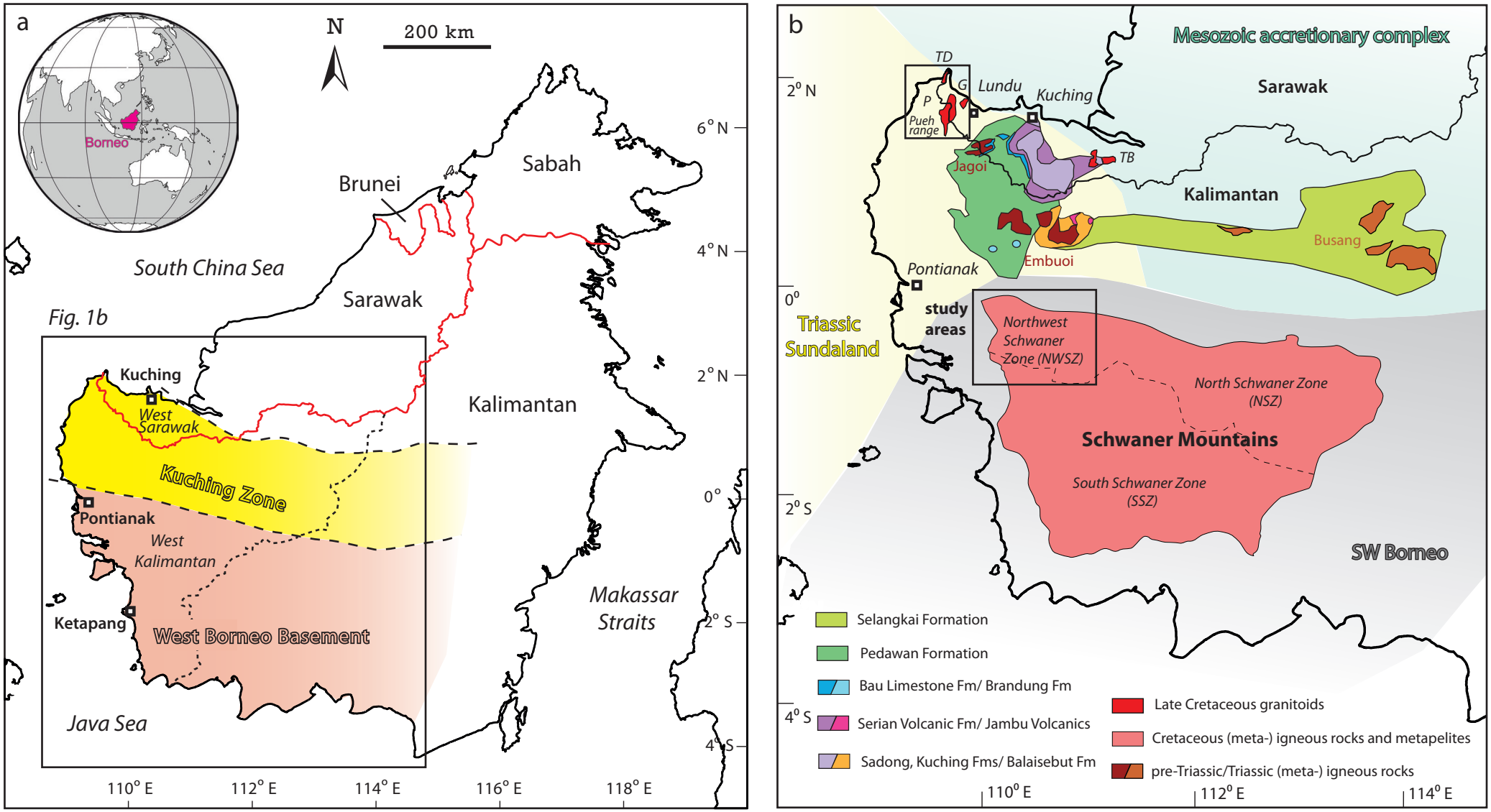
a
N
200 km
Borneo
Brunei
Sabah
South China Sea
Sarawak
Fig. 1b
Kalimantan
Kuching
West Sarawak
Kuching Zone
Pontianak
West Kalimantan
Ketapang
West Borneo Basement
Java Sea
Makassar Straits
6° N
4° N
2° N
0°
2° S
4° S
110° E
112° E
114° E
116° E
118° E
b
Mesozoic accretionary complex
TD
G
P
Pueh range
Lundu
Kuching
Sarawak
Jagoi
TB
Kalimantan
Busang
Embuoi
Pontianak
study areas
Triassic Sundaland
Northwest Schwaner Zone (NWSZ)
North Schwaner Zone (NSZ)
Schwaner Mountains
South Schwaner Zone (SSZ)
SW Borneo
2° N
0°
2° S
4° S
Selangkai Formation
Pedawan Formation
Bau Limestone Fm/ Brandung Fm
Serian Volcanic Fm/ Jambu Volcanics
Sadong, Kuching Fms/ Balaisebut Fm
Late Cretaceous granitoids
Cretaceous (meta-) igneous rocks and metapelites
pre-Triassic/Triassic (meta-) igneous rocks
110° E
112° E
114° E

Fig. 1

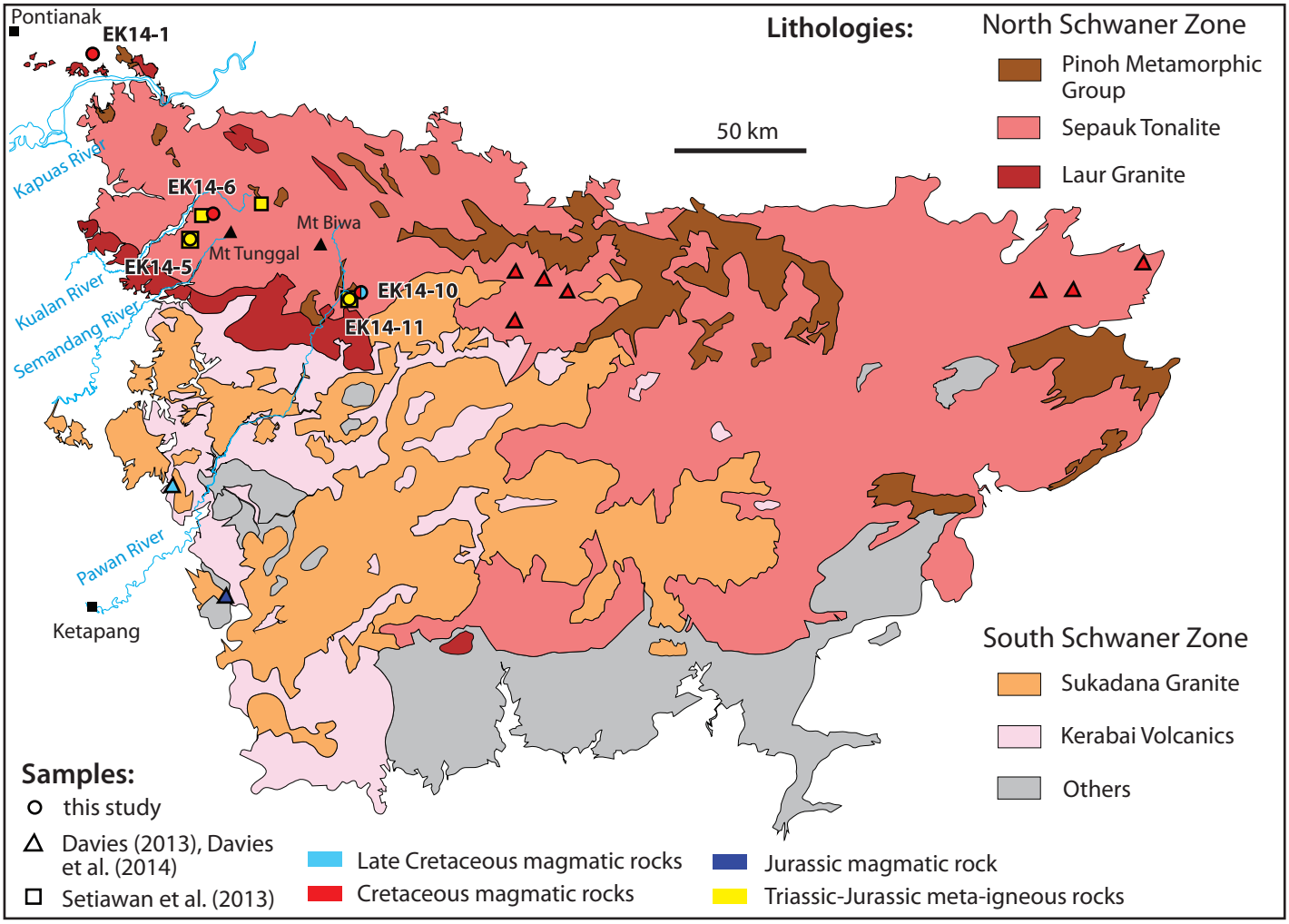
Pontianak
EK14-1
Kapuas River
EK14-6
Mt Biwa
Mt Tunggal
EK14-5
Kualan River
Semandang River
EK14-10
EK14-11
Pawan River
Ketapang
50 km
Lithologies:
North Schwaner Zone
Pinoh Metamorphic Group
Sepauk Tonalite
Laur Granite
South Schwaner Zone
Sukadana Granite
Kerabai Volcanics
Others
Samples:
this study
Davies (2013), Davies et al. (2014)
Setiawan et al. (2013)
Late Cretaceous magmatic rocks
Cretaceous magmatic rocks
Jurassic magmatic rock
Triassic-Jurassic meta-igneous rocks

Fig. 2

Fig. 3

Fig. 4

Fig. 5

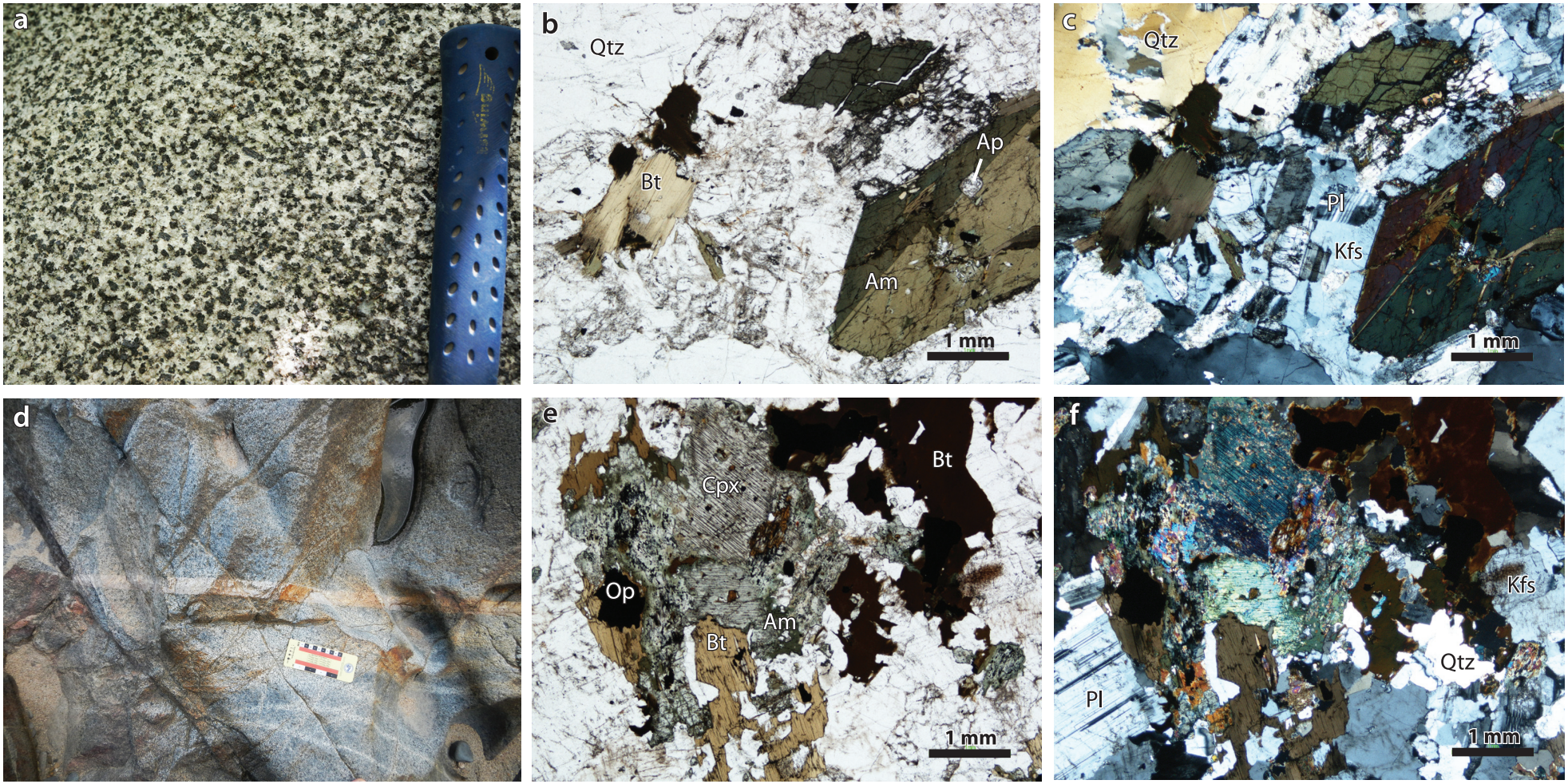
a
b
Qtz
Ap
Bt
Am
1 mm
c
Qtz
Pl
Kfs
1 mm
d
e
Bt
Cpx
Op
Am
Bt
1 mm
f
Kfs
Qtz
Pl
1 mm

Fig. 6


a
b
c
Spl+Wmca
Bt
Bt
1 mm
d
Spl+Wmca
Qtz
Pl
Pl
Qtz
1 mm
e
Qtz
Am
Pl
Kfs
Am
1 mm
f
1 mm

Fig. 7

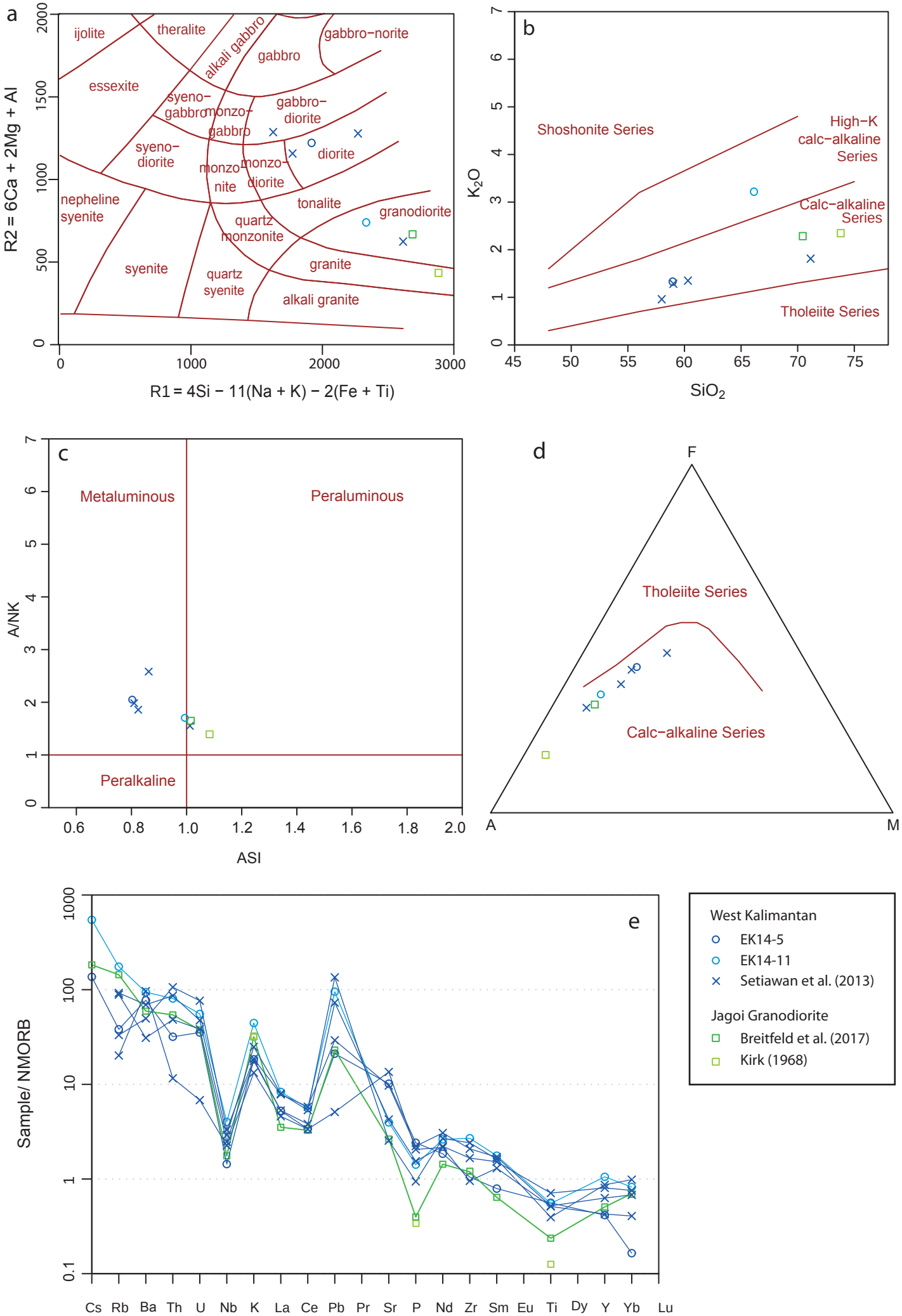
a
ijolite
theralite
alkali gabbro
gabbro–norite
gabbro
essexite
syeno–gabbro
monzo–gabbro
gabbro–diorite
diorite
syeno–diorite
monzo–diorite
monzo–nite
nepheline syenite
tonalite
granodiorite
quartz monzonite
syenite
granite
quartz syenite
alkali granite
R2 = 6Ca + 2Mg + Al
R1 = 4Si − 11(Na + K) − 2(Fe + Ti)
b
Shoshonite Series
High–K calc–alkaline Series
Calc–alkaline Series
Tholeiite Series
K2O
SiO2
c
Metaluminous
Peraluminous
Peralkaline
A/NK
ASI
d
F
Tholeiite Series
Calc–alkaline Series
A
M
e
Sample/ NMORB
Cs Rb Ba Th U Nb K La Ce Pb Pr Sr P Nd Zr Sm Eu Ti Dy Y Yb Lu
West Kalimantan
EK14-5
EK14-11
Setiawan et al. (2013)
Jagoi Granodiorite
Breitfeld et al. (2017)
Kirk (1968)

Fig. 8

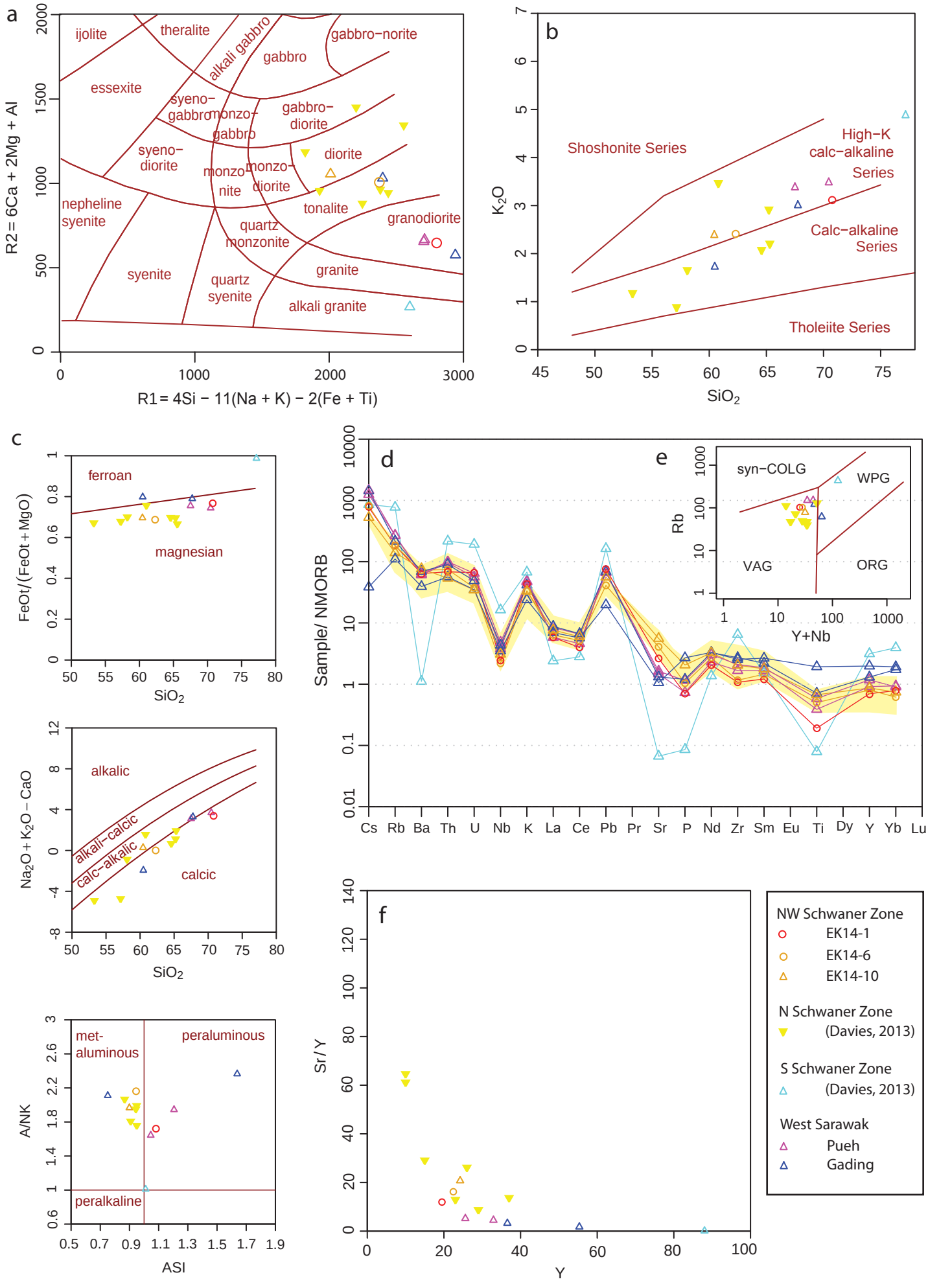
a
ijolite
theralite
alkali gabbro
gabbro
gabbro–norite
essexite
syeno–gabbro
monzo–gabbro
gabbro–diorite
syeno–diorite
diorite
monzo–nite
monzo–diorite
nepheline syenite
tonalite
granodiorite
quartz monzonite
syenite
quartz syenite
granite
alkali granite
R2 = 6Ca + 2Mg + Al
R1 = 4Si − 11(Na + K) − 2(Fe + Ti)
b
Shoshonite Series
High–K calc–alkaline Series
Calc–alkaline Series
Tholeiite Series
K2O
SiO2
c
ferroan
magnesian
FeOt/(FeOt + MgO)
SiO2
alkalic
alkali–calcic
calc–alkalic
calcic
Na2O + K2O − CaO
SiO2
met–aluminous
peraluminous
peralkaline
A/NK
ASI
d
Sample/ NMORB
Cs Rb Ba Th U Nb K La Ce Pb Pr Sr P Nd Zr Sm Eu Ti Dy Y Yb Lu
e
syn–COLG
WPG
VAG
ORG
Rb
Y+Nb
f
Sr/Y
Y
NW Schwaner Zone
EK14-1
EK14-6
EK14-10
N Schwaner Zone
(Davies, 2013)
S Schwaner Zone
(Davies, 2013)
West Sarawak
Pueh
Gading

Fig. 9

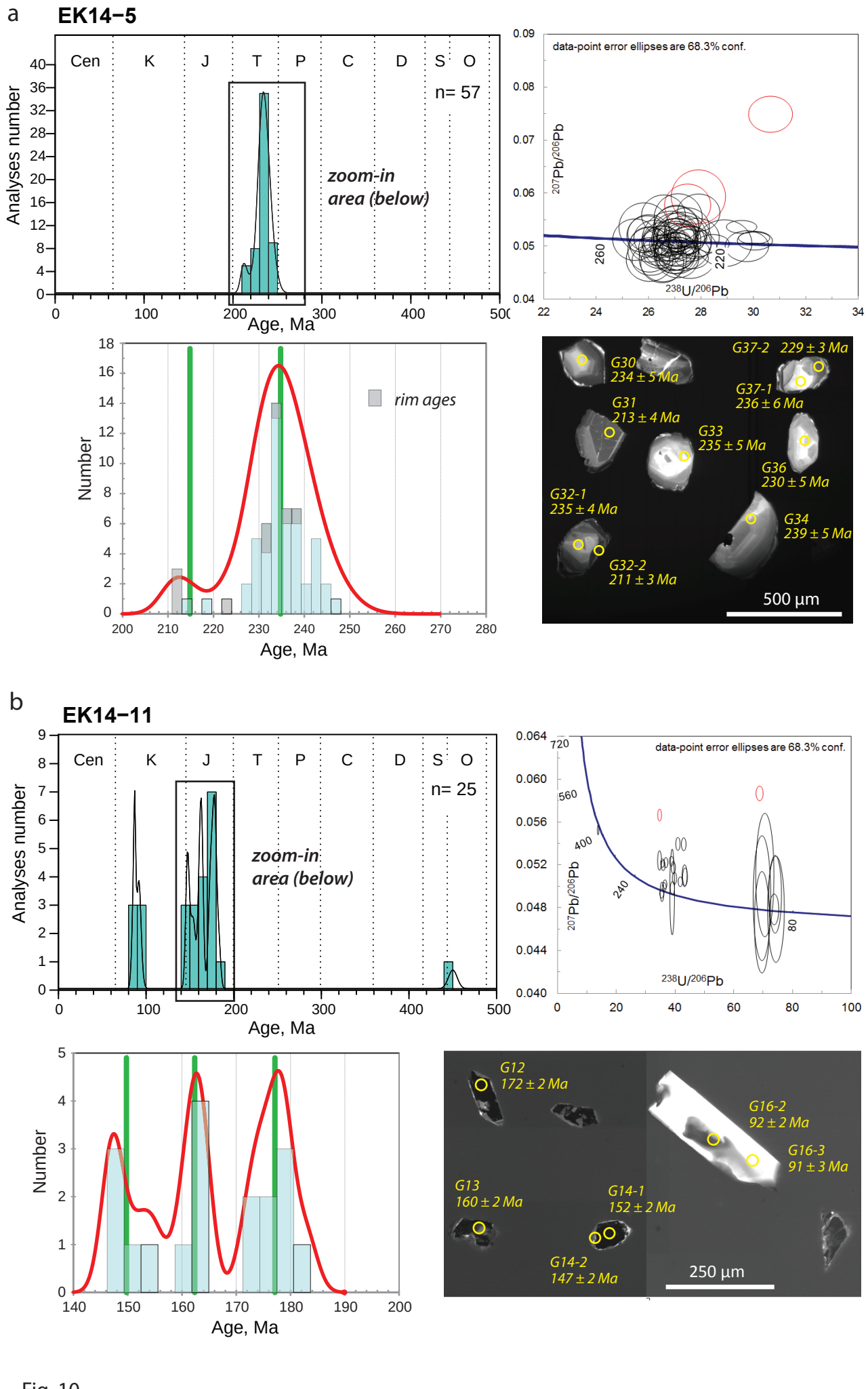
a
EK14−5
Cen
K
J
T
P
C
D
S
O
n= 57
zoom-in
area (below)
Analyses number
Age, Ma
data-point error ellipses are 68.3% conf.
207Pb/206Pb
238U/206Pb
260
220
rim ages
Number
Age, Ma
G30
234 ± 5 Ma
G37-2 229 ± 3 Ma
G37-1
236 ± 6 Ma
G31
213 ± 4 Ma
G33
235 ± 5 Ma
G36
230 ± 5 Ma
G32-1
235 ± 4 Ma
G34
239 ± 5 Ma
G32-2
211 ± 3 Ma
500 µm
b
EK14−11
Cen
K
J
T
P
C
D
S
O
n= 25
zoom-in
area (below)
Analyses number
Age, Ma
data-point error ellipses are 68.3% conf.
207Pb/206Pb
238U/206Pb
720
560
400
240
80
Number
Age, Ma
G12
172 ± 2 Ma
G16-2
92 ± 2 Ma
G16-3
91 ± 3 Ma
G13
160 ± 2 Ma
G14-1
152 ± 2 Ma
G14-2
147 ± 2 Ma
250 µm

Fig. 10

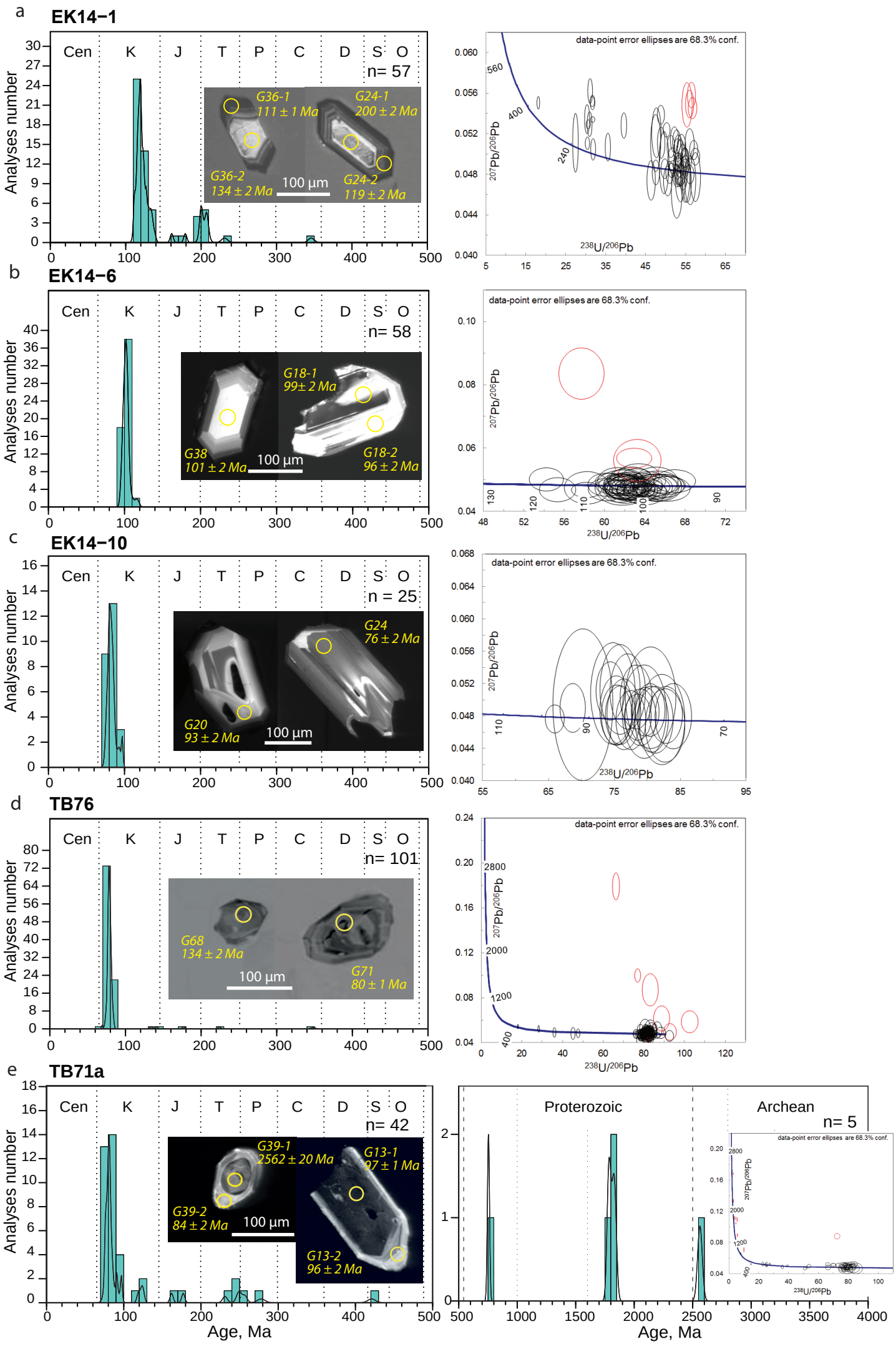
a
EK14−1
Cen K J T P C D S O
n= 57
Analyses number
G36-1
111 ± 1 Ma
G24-1
200 ± 2 Ma
G36-2
134 ± 2 Ma
100 µm
G24-2
119 ± 2 Ma
data-point error ellipses are 68.3% conf.
207Pb/206Pb
238U/206Pb
b
EK14−6
Cen K J T P C D S O
n= 58
Analyses number
G18-1
99± 2 Ma
G38
101 ± 2 Ma
100 µm
G18-2
96 ± 2 Ma
data-point error ellipses are 68.3% conf.
207Pb/206Pb
238U/206Pb
c
EK14−10
Cen K J T P C D S O
n = 25
Analyses number
G24
76 ± 2 Ma
G20
93 ± 2 Ma
100 µm
data-point error ellipses are 68.3% conf.
207Pb/206Pb
238U/206Pb
d
TB76
Cen K J T P C D S O
n= 101
Analyses number
G68
134 ± 2 Ma
100 µm
G71
80 ± 1 Ma
data-point error ellipses are 68.3% conf.
207Pb/206Pb
238U/206Pb
e
TB71a
Cen K J T P C D S O
n= 42
Analyses number
G39-1
2562 ± 20 Ma
G13-1
97 ± 1 Ma
G39-2
84 ± 2 Ma
100 µm
G13-2
96 ± 2 Ma
Age, Ma
Proterozoic
Archean
n= 5
data-point error ellipses are 68.3% conf.
207Pb/206Pb
238U/206Pb
Age, Ma

Fig. 11

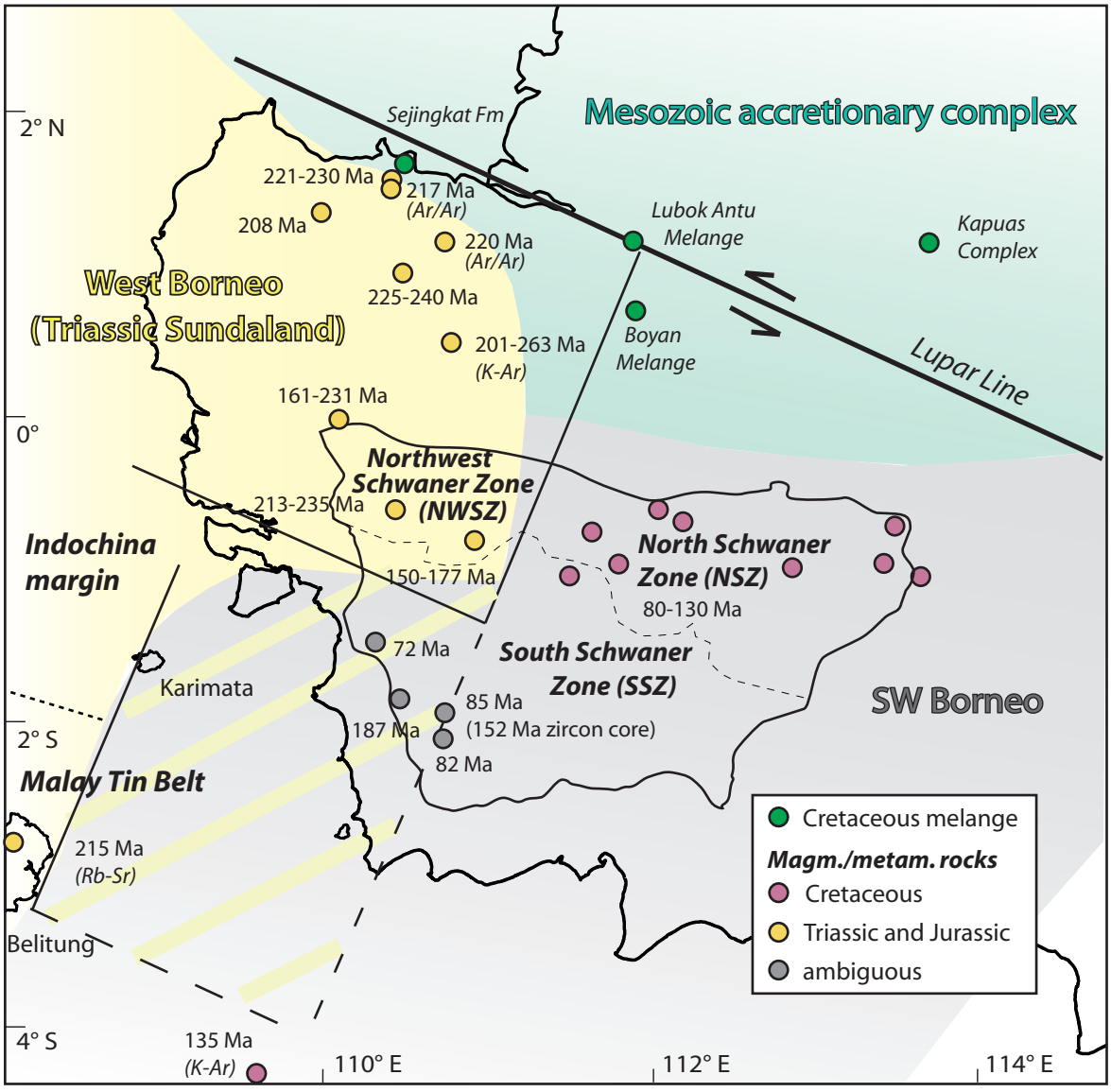
Mesozoic accretionary complex
Sejingkat Fm
2° N
221-230 Ma
217 Ma
(Ar/Ar)
208 Ma
220 Ma
(Ar/Ar)
Lubok Antu
Melange
Kapuas
Complex
West Borneo
(Triassic Sundaland)
225-240 Ma
201-263 Ma
(K-Ar)
Boyan
Melange
Lupar Line
161-231 Ma
0°
Northwest
Schwaner Zone
(NWSZ)
213-235 Ma
Indochina
margin
North Schwaner
Zone (NSZ)
150-177 Ma
80-130 Ma
72 Ma
South Schwaner
Zone (SSZ)
Karimata
85 Ma
(152 Ma zircon core)
187 Ma
82 Ma
SW Borneo
2° S
Malay Tin Belt
215 Ma
(Rb-Sr)
Belitung
4° S
135 Ma
(K-Ar)
110° E
112° E
114° E
Cretaceous melange
Magm./metam. rocks
Cretaceous
Triassic and Jurassic
ambiguous

Fig. 12

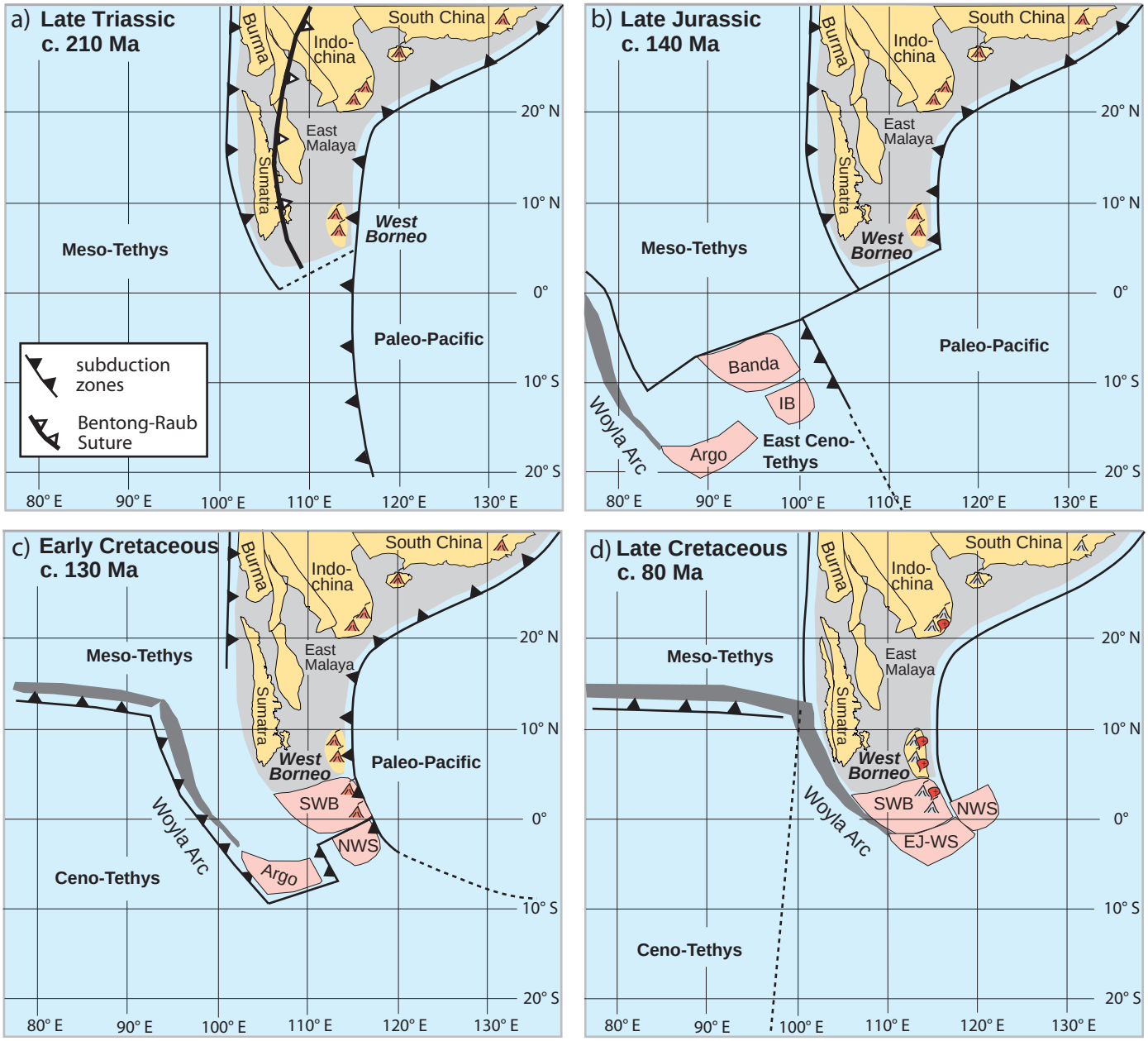
a) Late Triassic
c. 210 Ma
Burma
Indo-
china
South China
East
Malaya
Sumatra
West
Borneo
Meso-Tethys
Paleo-Pacific
subduction
zones
Bentong-Raub
Suture
b) Late Jurassic
c. 140 Ma
Banda
IB
Argo
Woyla Arc
East Ceno-
Tethys
c) Early Cretaceous
c. 130 Ma
SWB
NWS
Ceno-Tethys
d) Late Cretaceous
c. 80 Ma
EJ-WS
20° N
10° N
0°
10° S
20° S
80° E
90° E
100° E
110° E
120° E
130° E

Fig. 13

	West Kalimantan					West Sarawak			
Group	Meta-igneous	Meta-igneous	Igneous	Igneous	Igneous	Igneous	Igneous	Igneous	Igneous
Sample	**EK14-5**	**EK14-11**	**EK14-1**	**EK14-6**	**EK14-10**	**TB76**	**TB80**	**TB69**	**TB71a**
Lithology	D	GRD	GRD	T	D	GRD	GRD	T	GRD
SiO_2	58.96	66.15	70.78	62.32	60.44	70.46	67.50	60.48	67.76
TiO_2	0.71	0.70	0.24	0.63	0.85	0.49	0.74	2.44	0.90
Al_2O_3	17.45	15.33	14.75	16.12	16.74	14.38	14.71	12.68	15.32
Fe_2O_3	6.12	4.46	2.54	5.96	6.11	3.59	5.46	10.83	6.25
MnO	0.08	0.08	0.06	0.10	0.11	0.06	0.08	0.14	0.08
MgO	2.02	1.23	0.69	2.44	2.41	1.11	1.59	2.47	1.50
CaO	7.28	3.54	2.85	5.36	5.71	2.81	2.64	6.19	1.67
Na_2O	4.30	3.35	3.15	2.95	3.61	3.03	2.37	2.52	1.96
K_2O	1.33	3.22	3.12	2.41	2.39	3.48	3.38	1.73	3.01
P_2O_5	0.28	0.17	0.08	0.12	0.24	0.09	0.13	0.31	0.14
SO_3	0.03	0.03	0.02	0.03	0.03	0.02	0.03	0.02	0.02
Total	98.57	98.24	98.30	98.44	98.65	99.51	98.64	99.81	98.60
LOI	0.34	0.44	0.79	0.61	0.57	0.67	0.97	0.37	2.71
Ni	10	5	6	9	10	8	18	13	18
Cr	7	4	4	12	15	21	42	18	41
V	106	65	30	141	120	49	95	391	123
Sc	9	15	7	17	16	11	15	33	20
Cu	21	4	3	48	55	11	23	39	26
Zn	29	44	34	60	69	44	78	71	83
Ga	19	17	13	16	18	16	17	19	18
Pb	6	29	23	12	17	20	20	6	21
Sr	914	356	237	366	502	132	147	95	118
Rb	21	98	103	101	78	149	150	62	121
Ba	487	592	403	457	481	384	400	247	436
Zr	78	199	79	86	151	123	155	188	200
Nb	3	9	6	5	7	9	11	8	10
Ta	<0.4	<0.4	0.6	<0.4	<0.4	0.7	0.8	<0.4	1.2
Mo	<0.3	<0.3	<0.3	<0.3	0.6	<0.3	0.5	2.0	0.4
Th	4	10	8	9	6	11	12	7	11
U	1.7	2.6	3.1	1.8	1.6	2.6	3.0	1.6	2.3
Y	12	30	20	22	24	26	33	55	37
La	13	21	15	16	19	15	21	17	22
Ce	25	42	30	39	45	34	49	43	50
Nd	13	19	15	20	24	17	22	24	24
Sm	2.1	4.6	3.2	3.8	4.7	4.4	4.9	7.0	5.8
Yb	<0.8	2.5	2.4	1.9	2.3	2.9	2.8	5.9	5.3
Cs	<2	4	5	6	4	9	10	<2	10

All iron is measured as Fe_2O_3. LOI = loss on ignition (wt %). Oxides in wt %; elements in ppm.

D = diorite; T = tonalite; GRD = granodiorite.

Tab. 1